

Fall 2019

The Biogeochemical Behavior and Speciation of Mercury in the Sea Surface Microlayer: Implications for Transport to Watersheds via Fog

Alexander J. Olson
California State University, Monterey Bay

Follow this and additional works at: https://digitalcommons.csumb.edu/caps_thes_all

Recommended Citation

Olson, Alexander J., "The Biogeochemical Behavior and Speciation of Mercury in the Sea Surface Microlayer: Implications for Transport to Watersheds via Fog" (2019). *Capstone Projects and Master's Theses*. 654.

https://digitalcommons.csumb.edu/caps_thes_all/654

This Master's Thesis (Open Access) is brought to you for free and open access by the Capstone Projects and Master's Theses at Digital Commons @ CSUMB. It has been accepted for inclusion in Capstone Projects and Master's Theses by an authorized administrator of Digital Commons @ CSUMB. For more information, please contact digitalcommons@csumb.edu.

THE BIOGEOCHEMICAL BEHAVIOR AND SPECIATION OF MERCURY
IN THE SEA SURFACE MICROLAYER: IMPLICATIONS FOR
TRANSPORT TO WATERSHEDS VIA FOG

A Thesis

Presented to the

Faculty of

Moss Landing Marine Laboratories

California State University Monterey Bay

In Partial Fulfillment

of the Requirements for the Degree

Master of Science

in

Marine Science

by

Alexander J. Olson

Fall 2019

CALIFORNIA STATE UNIVERSITY MONTEREY BAY

The Undersigned Faculty Committee Approves the

Thesis of Alexander J. Olson:


The Biogeochemical Behavior and Speciation of Mercury in the Sea Surface

Microlayer: Implications for Transport to Watersheds via Fog

Kenneth H. Coale, Chair
Moss Landing Marine Laboratories

Carl H. Lamborg
University of California, Santa Cruz

Tom Connolly
Moss Landing Marine Laboratories

Approved by the Dean of Graduate Studies 

Kris Roney, Dean
Associate VP for Academic Programs and Dean of Undergraduate and Graduate Studies

12/17/2019

Approval Date

Copyright © 2019

by

Alexander J. Olson

All Rights Reserved

DEDICATION

For

Nicholas Yakas

Christopher Yakas

James Yakas

Jim Yakas

Mary Yakas

Angie Clark

Richard Ternullo

Yvonne Silva

Tyrone McGraw

Thank you for the precious gift of perspective.

“A human being should be able to change a diaper, plan an invasion, butcher a hog, conn a ship, design a building, write a sonnet, balance accounts, build a wall, set a bone, comfort the dying, give orders, take orders, cooperate, act alone, solve equations, analyze a new problem, pitch manure, program a computer, cook a tasty meal, fight efficiently, die gallantly. Specialization is for insects”

- Robert Heinlein, 1973

“The Northmen did not grumble at this, for they are cheerful at all times; I alone grumbled, and mightily. They paid me no attention.

Finally I said to Herger, ‘The rain is cold.’

To this he laughed. ‘How can the rain be cold?’ he said. ‘You are cold and you are unhappy. The rain is not cold or unhappy.’”

- Michael Crichton, *Eaters of the Dead: The Manuscript of Ibn Fadlan Relating his Experiences with the Northmen in AD 922*

ABSTRACT

The Biogeochemical Behavior and Speciation of Mercury in the Sea Surface Microlayer:
Implications for Transport to Watersheds via Fog

By

Alexander J. Olson
Master of Science
California State University Monterey Bay, 2018

Neurotoxic monomethylmercury (MMHg) found in coastal Central California marine advective fog is thought to be a source of elevated MMHg levels throughout the terrestrial coastal foodweb. While not currently present at hazardous concentrations for human exposure directly (17-54 pM), MMHg in fog along the coast poses potential health and ecosystem threats via food-web bioaccumulation and biomagnification processes. The likely marine source and the mechanism of its transport remain unknown.

While 2014 vertical profiles from coastal California show surface waters (<6 m) relatively deplete in MMHg (25-185 fM), similar to other ocean basins, surface grab sampling revealed elevated concentrations of MMHg in the uppermost (top ~100µm) portion of the water column known as the surface microlayer (SML). When corrected for dilution during sampling, this could represent a SML concentration of MMHg as high as 1.3 nM, orders of magnitude greater than the localized seawater and fog water; as well as the first such known measurements.

Further refined sampling in 2015 of nearshore and offshore waters of California and Oregon supported 2014 findings, with underlying bulk water and SML concentrations from 16 - 380 fM and 4 – 48 fM respectively (Enrichment factors (EF) of 2.5 – 30). These are the first such measurements of MMHg in the SML to our knowledge. SML concentrations were highly variable, likely due to the variable and patchy nature of the SML and its constituents. This may also account for little variability among different surface areas of glass sampling methods. While not statistically significant, these EFs trend with certain oceanographic conditions (temperature, solar radiation, and fluorescence [Chl-a proxy]) suggesting photodegradation and or photodemethylation as major factors affecting enrichment.

Although limited, bubble induced SML sea spray aerosol (SSA) production, and thus the ejection of MMHg into the atmosphere as fog nuclei, was also shown to be a potential contributing mechanism to MMHg in fog. Incubation experiments of acidified bulk seawater points to acidolysis of gaseous Dimethylmercury (DMHg) into MMHg as the major pathway of MMHg into regional marine advective fog. Continued comprehensive monitoring via California coastal fog sampling sites (FogNet) and coastal marine features and processes are needed to establish and discern changes in spatio-temporal patterns of the MMHg marine-terrestrial flux.

TABLE OF CONTENTS

	PAGE
ABSTRACT.....	vi
LIST OF TABLES.....	viii
LIST OF FIGURES	ix
ACKNOWLEDGEMENTS.....	xi
 CHAPTER	
1 MONOMETHYLMERCURY IN FOG.....	1
Methods.....	7
Results & Discussion	12
2 THE SEA SURFACE MICROLAYER (SML).....	20
Methods.....	23
Results & Discussion	31
3 FOG MMHG VIA DMHG ACIDOLYSIS.....	49
Methods.....	53
Results & Discussion	53
CONCLUSION.....	57
REFERENCES	60
APPENDIX A.....	72

LIST OF TABLES

	PAGE
Table 1. Literature Estimates of Primary Hg to the Environment	1
Table 2. Major Mercury Species and Properties.....	4
Table 3. Sediment-Water Diffusive Flux Estimates for Shelf Stations	17
Table 4. 2015 SML MMHg Enrichment Factors & Oceanographic Parameters ..	32
Table 5. SML Trace Metal Enrichment Factors in the Marine Environment	36
Table 6. SML MMHg & THg Enrichment Factors and MMHg:THg	42

LIST OF FIGURES

	PAGE
Figure 1. Atmospheric Mercury Emissions From Coal Combustion	2
Figure 2. Literature Estimates of Primary Hg to the Environment.....	5
Figure 3. Representative Profiles of Monomethylmercury and Total Methylated Mercury in Seawater	5
Figure 4. 2014-2015 Study Sites.....	8
Figure 5. At Sea Analysis of Volatile Gaseous Hg Species (DMHg & Hg ⁰)	9
Figure 6. At Sea MMHg Analysis	10
Figure 7. 2014 SML Grab Sampling.....	12
Figure 8. Hg ⁰ & THg Shelf Profiles.....	13
Figure 9. DMHg & MMHg Shelf profiles	14
Figure 10. Hg ⁰ & THg Offshore Profiles.....	15
Figure 11. DMHg & MMHg Offshore Profiles	16
Figure 12. MMHg SML Surface Grabs vs Underlying Water.....	18
Figure 13. Diluted vs Undiluted MMHg SML Grabs.....	19
Figure 14. Conceptual Model of the Sea Surface Microlayer	21
Figure 15. MMHg and MMHg:THg in Coastal Fog	22
Figure 16. 2014-2015 Cruise, Fog & SML Stations.....	24
Figure 17. SML Glass Samplers	25
Figure 18. Aerosol Generator	28
Figure 19. Sea Spray Collection	29
Figure 20. Open Ocean SML MMHg Enrichment Factors.....	32
Figure 21. Enrichment Factor Trends with Oceanographic Parameters	33
Figure 22. Eddy SML MMHg	34
Figure 23. Microplastics in the Marine Foodweb	37
Figure 24. MMHg in Coastal Compartments	38
Figure 25. SML Methods Comparison	40
Figure 26. February 2018 SML MMHg & THg Enrichment Factors.....	41
Figure 27. Percent MMHg of THg in SML & UW	42
Figure 28. MMHg/Cl ⁻ Ratios Across Coastal Compartments	44
Figure 29. Chl-a in the SML & UW	45
Figure 30. Chl-a & Phaeopigments Fractions with MMHg in the SML & UW....	46

Figure 31. SML and UW PAH & CDOM vs MMHg.....	48
Figure 32. DMHg Profiles in Offshore Eddies	50
Figure 33. DMHg Profiles in Monterey Bay	51
Figure 34. DMHg Stability By Container Type, Temperature & Light	52
Figure 35. DMHg & MMHg in Sparged and Acidified Samples	52
Figure 36. DMHg Loss in Acidified Seawater Incubations.....	54
Figure 37. Apparent DMHg to MMHg Conversion	54
Figure 38. Psuedo First Order DMHg Demethylation Rate Constant	55
Figure 39. Dimethyl Sulfide Propionate (DMSP) into the MBL.....	56
Figure 40. Conceptual Model of Hg Cycling in the California Coastal Zone	59

ACKNOWLEDGEMENTS

Thankful and indebted to Kenneth Coale for what I can only describe as being the grandfather(s) I never had, and to Tom Connolly and Carl Lamborg for their guidance, patience and expertise in helping create this thesis. I count myself so fortunate to have family and friends whose support and understanding of my journey means more than I can ever put into words. Jim Harvey and Diana Steller, thank you for the cold foggy mornings in wetsuits and on whalers, and the countless relationships and opportunities that stemmed from these long field days. To the countless people who cheered and inspired me before to get here, again I am thankful and speechless.

Mar Ops, Brian, JD, Jackson, Kate: Thank you for all the dirty hands, sweat and water time that was good for the soul. It kept me sane and afloat.

MPSL, Wes, Amy, Adam, Autumn, Billy, Steve, Chris, Melissa, Jessica and Jessica: Some of my samples would have been lost to time or not collected at all, and I owe so much to all your skills.

Thanks to my haphazardly assembled whaler crews, labmates and enablers who made my data possible: Holly Chiswell, Katie Graves, Mo Wise, Emmet Haggard, Justin Cordova, Rachel Brooks, Jenni Johnson, Amber Reichert, Phillip Reyes, Chris Beebe, Sharon Hsu, Kim Elson, Laurel Lam & Fam, Jason Adelaars Kenji Soto, Vivian Ton and Sierra Helmann.

CHAPTER 1

Monomethylmercury in Fog

Introduction

Mercury (Hg) is a pervasive heavy metal occurring at trace concentrations in the Earth's crust. Hg emanates from the crust to the hydrosphere and atmosphere via natural primary sources such as volcanoes, calderas, and other geothermal vents, with fluxes estimated at $\sim 200 \text{ Mg/yr}^{-1}$ (Pirrone *et al.*, 2010; Driscoll *et al.*, 2013; Amos *et al.*, 2015, Table 1). Due to its unique physico-chemical properties, Hg has been used for a wide variety of applications throughout history, thus exacerbating the natural flux of this

Table. 1 Literature Estimates of Primary Hg to the Environment (Amos et al., 2015)

source	annual release (Mg year^{-1})	cumulative release (Gg)
Geogenic		
emissions to the atmosphere		
volcanoes, passive degassing	76 ± 30^b $\sim 100^d$	12 ± 5^c $\sim 16^c$
volcanoes, large sporadic eruptions	2000–5000 Mg per event ^e	$>4^f$
geothermal	60^g	9.6^c
releases to water		
sea floor hydrothermal vents	$<20^h$	$<3.2^c$
Anthropogenic		
emissions to the atmosphere		
2005	1900^i , 2000^j	
2008	2000 (1300 – 3200) ^k , 1300^l	
2010	2000 (1000 – 4100) ^m , 1600^n , 2400^o	
since 1850		220 (140 – 370) ^{k,p} , 320^o
all time		350 (230 – 790) ^{k,p}
releases to land and water		
2010	1100 (550 – 1900) ^{m,q} , $1400^{o,r}$	
since 1850		$310^{o,s}$

^aPyle and Mather⁶¹ estimate small sporadic volcanic eruptions release 500 (60 – 2000) Mg of Hg year^{-1} . Emissions from geologically enriched soils along the world's mercuriferous belts have been estimated to be between 500 and 750 Mg year^{-1} .⁶⁴ The analysis here suggests these may be overestimated based on empirical constraints on the global Hg cycle (see Figure 4 and text in Section 3.0). ^bBagnato et al.⁶⁰ ^cAssuming a constant emission rate between 1850 and 2010. ^dBagnato et al.,⁵⁹ Mather et al.,¹¹⁷ Andren and Nriagu² ^ePyle and Mather⁶¹ ^fFor four large eruptions between 1850 and 2010. Large eruptions occur at a frequency of 1–2 times per century. ^gVarekamp and Buseck¹¹⁸ ^hLamborg et al.⁶³ for total dissolved Hg (and MMHg) inputs. ⁱWilson et al.¹¹⁹ ^jPacyna et al.¹²⁰ ^kStreets et al.¹⁹ ^lMuntean et al.¹²¹ ^mAMAP/UNEP¹²² ⁿRafaj et al.¹²³ ^oHorowitz et al.²⁰ Note this inventory includes commercial products missing from previous emission estimates. ^pRange represents 80% confidence intervals. ^qIncludes primary anthropogenic releases of 190 (range, 40–580) Mg year^{-1} to water, plus ASGM releases to land and water of 880 (range, 500–1300) Mg year^{-1} . ^rReleases to water are 560 Mg year^{-1} , and releases to land are 790 Mg year^{-1} . ^sCumulative releases to water are 160 Gg, and releases to land are 150 Gg.

element into the biosphere (Sun *et al.*, 2006; Horowitz *et al.*, 2014). The release of Hg as by products in energy production, combustion of coal in power plants, mining and manufacturing processes (such as smelting, dry-cell batteries and caustic soda (NaOH) production) account for much of the historic anthropogenic fluxes since the onset of the Industrial Revolution, as well as small- and large-scale artisanal gold mining extending as far back as 3000BC (Lamborg *et al.*, 2002; Amos *et al.*, 2013; Obrist *et al.*, 2018).

Globally the atmospheric flux of Hg has increased about 3-5-fold since ~1850, with the current estimated global atmospheric Hg reservoir at 4.4-5.3 Gg, an order of magnitude (15x) above natural levels. Anthropogenic emissions primarily originate from heavily populated and developing countries within Europe and Asia, particularly India and China, due to the increasing prevalence of coal-fired power plants (Fig. 1, Streets *et al.*, 2018).

Although the majority of Hg from power plants and industry is deposited locally (within 100 km), some Asian emissions and dust are transported globally by tropospheric winds across the Pacific Ocean to North America (Mason *et al.*, 1994). This long-range atmospheric transport and deposition, considered the largest sources of Hg transport and flux, reaches even the most remote areas making Hg pollution a truly global concern (Mason *et al.*, 1994; Driscoll *et al.*, 2013; Steding & Flegal, 2002).

Due to its lipophilic nature, methylated Hg is greatly bioaccumulated and biomagnified up the food web with factors of 10,000x to 100,000x from water to phytoplankton alone (1st trophic transition) (Fisher & Reinfelder, 1995; Pickhardt & Fisher, 2007; Lawson & Mason,

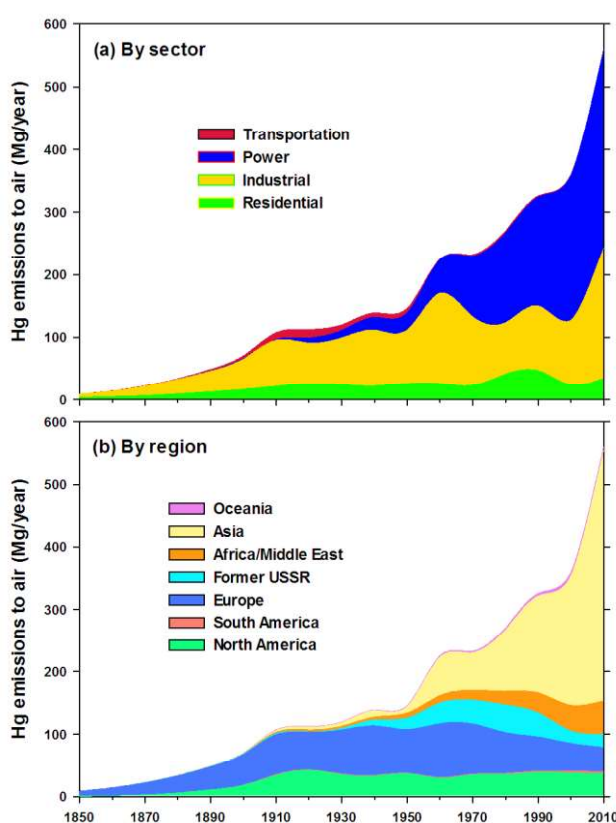


Figure 1. Atmospheric mercury emissions from coal combustion, 1850-2010, by sector (a) and world region (b). From Streets *et al.*, 2018

1998; Moye *et al.*, 2002). Thereafter, it increases by a factor of about 10 for each further trophic transfer, up to fish and birds (Scheuhammer, 1991; Mason *et al.*, 1996; Lasorsa *et al.*, 1995).

Onshore measurements of the neurotoxic species monomethylmercury (MMHg, CH_3Hg^+) in coastal Central California marine advective fog water show concentrations 100 times that of local rain, a previous subject of study for transpacific Hg pollution (Weiss-Pienzas *et al.*, 2012). Marine fog is a major source of water to the maritime chaparral complex and redwood forests and the animals and vegetation in these regions (Ingraham *et al.*, 1995; Dawson, 1998). Its association with elevated MMHg concentrations in ecosystem biota from the same geographical locations (Ortiz *et al.*, 2014; Rytuba, 2014), suggests marine fog as a transportation and consolidation mechanism for toxic marine mercury to the coastal terrestrial realm. While all Hg species can be toxic at varying concentrations, MMHg has been the cause of most mercury poisoning cases, primarily through the consumption of contaminated seafood (Renzoni *et al.*, 1998). This makes MMHg the greatest concern when compared to other Hg species in nature (Table 2, U.S. EPA. Integrated Risk Information System IRIS, 2001).

Natural and anthropogenic sources of elemental Hg (Hg^0) and MMHg are known to cycle throughout the marine and terrestrial environments, yet there is limited understanding of Hg reaction mechanisms at atmospheric interfaces with land and sea, which can determine Hg speciation and pathways (Ariya *et al.*, 2015; Subir *et al.*, 2012; Subir *et al.*, 2011).

Wet atmospheric deposition is the main source of Hg to the open ocean, mostly as oxidized, divalent Hg (Hg^{2+} or Hg (II)) (Mason *et al.*, 1994), while rivers are a dominant source to the coastal zone. Hg(II) can then be methylated, scavenged by sinking particles from the water column or reduced (biologically or photochemically) to Hg^0 and evade into the atmosphere (Fig. 2, Lamborg *et al.*, 2014). Losses of Hg^0 and Hg^{2+} from the water column appear to be gaseous evasion of Hg^0 to the atmosphere and particle transport of Hg^{2+} to the sediments. Continental shelf sediments, nearshore marshes, and

rivers provide sources to coastal waters, while sedimentation, biological uptake, photochemical decomposition, and advective transport offshore act as sinks (Lamborg *et al.*, 2014).

Table 2: Major mercury species and properties

Mercury Species	(Abbreviation) [seawater conc.]	Properties [vapor pressure]	Major Forms in Seawater
Elemental (Hg ⁰)	Hg ⁰ [18 – 115.2 fM] ^a	Silver liquid at most temperatures Volatile [0.002 mmHg] Toxic fumes 1/2 of Hg emissions ^b	Hg ⁰
Ionic (HgII)	Hg ²⁺ [<0.2 – 6.9pM] ^b	Highly reactive Short residence time 1/2 of Hg emissions ^b	HgCl ₂
Dimethyl- (DMHg)	(CH ₃) ₂ Hg [<10 – 670 fM] ^c	Neurotoxin, gas at room temperature Volatile [50-82 mmHg] ^d	(CH ₃) ₂ Hg
Monomethyl- (MMHg)	CH ₃ Hg ⁺ [<0.02 – 500 fM] ^c	Neurotoxin, readily passes into tissue Volatile [9 mmHg] ^e	CH ₃ HgCl CH ₃ Hg – ligand

^a Mason *et al.*, 2017 (Hg⁰ = 90% of dissolved gaseous mercury); ^b Morel *et al.*, 1994; ^c Gworek *et al.*, 2016;

^d Witt *et al.*, 1991; ^e Kim & Zoh, 2012;

MMHg production occurs under a specific set of redox conditions, initially documented in anoxic sediments harboring sulfate reducing bacteria (SRB) capable of methylating Hg as a byproduct of cellular metabolism (Compeau, 1985). However, unexplained microbial methylation has also been shown to occur in both oxic and relatively hypoxic environments in the open ocean, often in oxygen minimum zones (OMZs) within the water column (Fig. 3 Topping & Davies, 1981; Mason & Fitzgerald, 1993; Monperrus *et al.*, 2007; Heimbürger *et al.*, 2010; Lamborg *et al.*, 2014). More recent evidence suggests a larger group of potential methylating anaerobic bacteria than previously thought (Gilmour *et al.*, 2018; Gilmour *et al.*, 2011; Parks *et al.*, 2013).

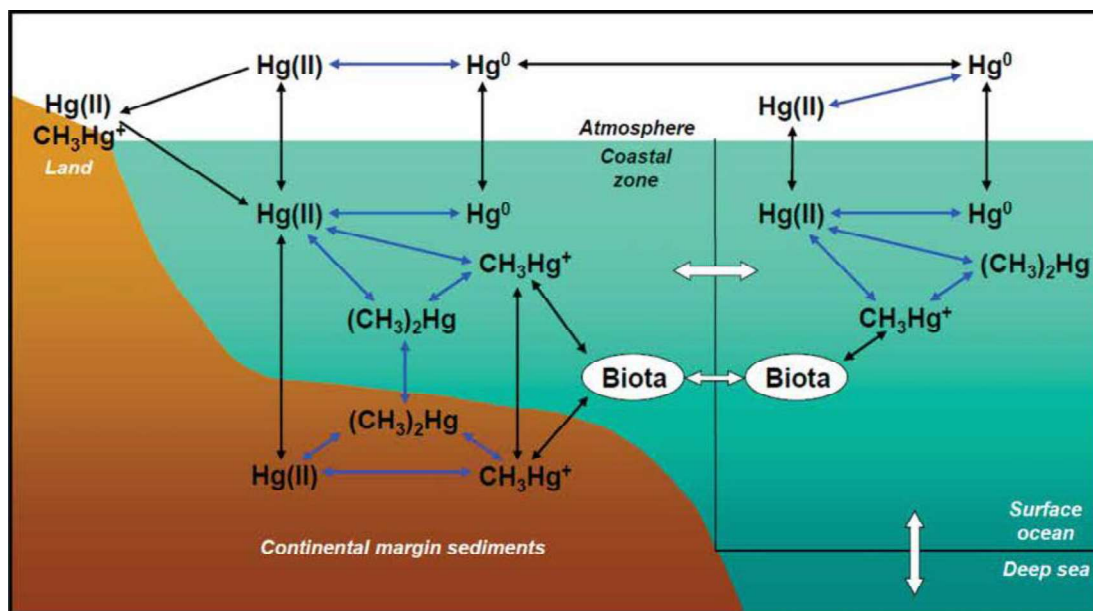


Figure 2. From Lamborg et al., 2014 “Conceptual model of mercury biogeochemical cycling in the ocean. Blue arrows highlight biogeochemical transformations of mercury. Black arrows denote fluxes among the atmosphere, water, sediments, and biota. All of the mercury species can be transported hydrologically between the coastal zone, surface ocean, and deep sea, with bioaccumulative CH_3Hg^+ also transported by bioadvection (white arrows; Fitzgerald et al., 2007).”

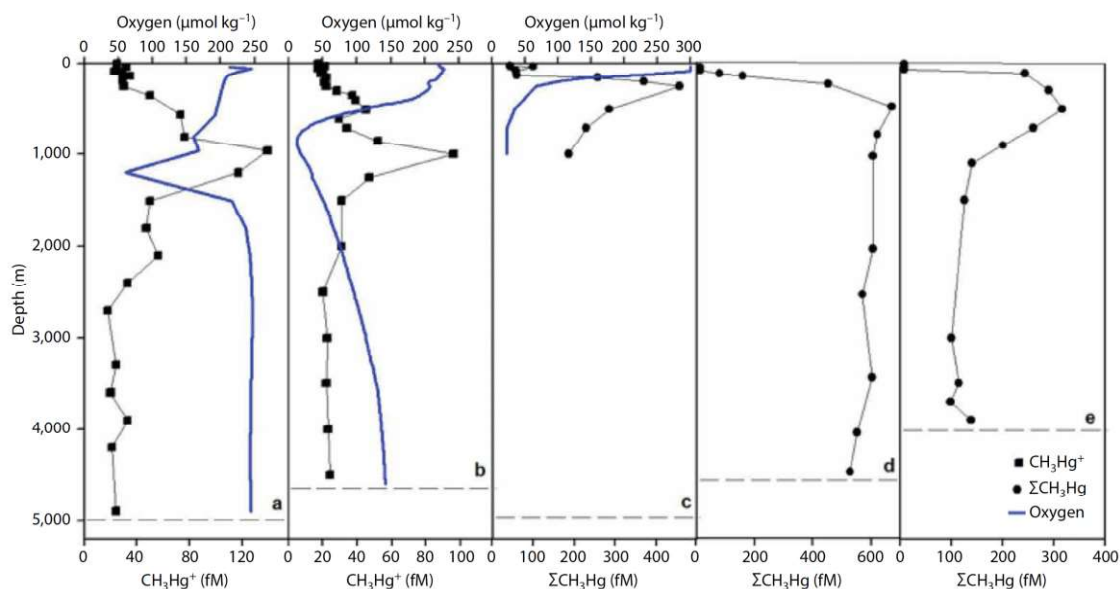


Figure 3. From Lamborg et al., 2014, “Representative profiles of monomethylmercury (CH_3Hg^+) and total methylated ($\Sigma\text{CH}_3\text{Hg}$) in seawater, illustrating a connection to dissolved oxygen distributions. Filtered CH_3Hg^+ in (a) Northeast Atlantic Ocean (recent work of author Bowman), and (b) subtropical North Pacific Ocean (Hammerschmidt and Bowman, 2012). $\Sigma\text{CH}_3\text{Hg}$ in unfiltered water of the (c) sub-Arctic North Pacific (Sunderland et al., 2009), (d) Southern Ocean (Cossa et al., 2011), and (e) Mediterranean Sea (Cossa et al., 2009). Dashed lines denote the depth of the sediment-water interface.”

Most Hg coastal studies have been conducted on the eastern seaboard of North America, a region characterized by a high density of coal fired power plants, with abundant riverine inputs and a wide continental shelf. California, however, is characterized by long range atmospheric sources (Asia), little fluvial input and a narrow shelf system.

In this study, we investigated coastal nearshore and offshore processes in the California Current System that may be responsible for a flux of MMHg to the lower troposphere, marine fog, and perhaps the production of MMHg within the air-sea boundary layer. Henry's Law Constant (a measure of volatility and solubility) for MMHg (1.6×10^{-5} , 15°C) compared to DMHg (646, 25°C) (Schroeder & Munthe, 1998) suggests MMHg to be much less likely to evade to the atmosphere as a gas (as DMHg does), and instead exist in a liquid or bound to a solid phase. Evasion of particulate or dissolved MMHg into fog would have to pass through the dynamic air-sea boundary zone, also known as the sea surface microlayer (SML). Working from the hypothesis that open ocean and coastal MMHg production was associated with anoxic environments and methylating bacteria, various microenvironments and reservoirs thought to be important for mercury flux were measured. Here we report the vertical distribution of MMHg and DMHg, total gaseous and total mercury in the southern, central and northern regions of the California Current. These profiles have been determined for nearshore stations over the continental shelf as well as in cyclonic and anticyclonic eddies within the offshore regions of the California Current. Sampling within cyclonic and anticyclonic mesoscale eddies afforded the advantage of being able to sample upwelling regions in the absence of the normal coastal wind-driven upwelling that characterizes the California Current from March through June. These include investigations of the possible formation of MMHg in coastal nearshore sediments, oxygen minima, and microenvironments such as plankton and the SML. The SML is of particular concern as it separates the marine realm from the earth's atmosphere.

METHODS

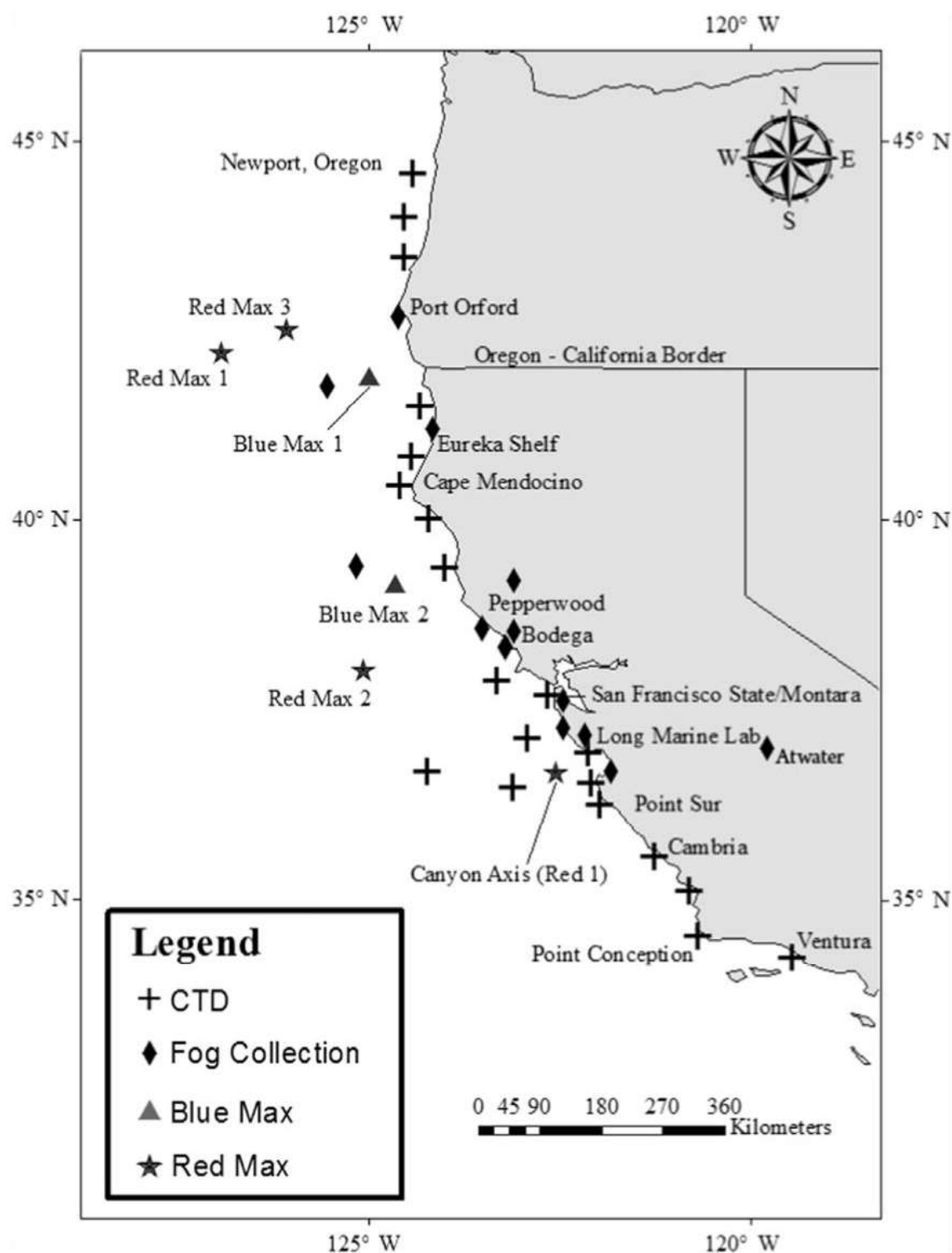
Study Site(s)

34 ocean sampling sites sampled during the summers of 2014 & 2015 extended from Ventura, California to Newport, Oregon (Fig. 4) aboard research vessels *R/V Point Sur* (June 2014, August 2014), *R/V Robert Gordon Sproul* (June 2015) and *R/V Oceanus* (August 2015). These cruises targeted various coastal and offshore compartments (water column, sediments, neuston and mesoscale surface anomalies). Stations were chosen to compliment FogNet terrestrial sites (Weiss-Penzias *et al.*, 2016) and mesoscale eddies. Eddies were detected using satellite altimetry, with near real time contoured images sent daily (Fig. 4). Compiled mean surface level anomalies from multiple satellites were distributed by Aviso (<http://www.aviso.altimetry.fr/>, Ssalto/Duacs). Data was imaged using Interactive Data Language®, a product of Exelis Visual Information Solutions, Inc. A number of stations were revisited over the 4 cruises (Appendix A).

Seawater

Bottle depths were chosen to capture features such as density gradients, maxima and minima in, chlorophyll, oxygen, turbidity, temperature, etc. During CTD casts attempts were made to trip bottles as close to the sediments as possible. This was always weather and operator dependent but usually within 2 to 5 meters of the bottom. Dimethyl mercury (DMHg) and total gaseous mercury were determined on board, whereas both MMHg and total mercury samples were returned to the lab for subsequent analysis. To test whether photodemethylation or acidolysis of DMHg may be occurring in surface seawater and in the more acidic fog water fraction, THg, MMHg and DMHg seawater samples for water column profiles were collected from 10 liter Niskin bottles deployed on a CTD rosette and lowered on conducting hydrowire from research vessels in 2015. The bottles were acid cleaned, rinsed with MQ water and had silicone internal closures to minimize metal contamination from springs or rubber. Sampling blanks were determined by filling the Niskin bottles with MQ water for a period of one hour, then sampling the bottles in the same way that seawater samples were processed. DMHg and Gaseous Elemental Mercury (GEM) analysis used modified techniques described in Bowman &

Figure 4. Fog collection stations on land and at sea (diamond), as well as hydrographic (CTD collections) (+) stations along coastal Oregon and California. Red Max and Blue Max refer to upwelling (blue) and downwelling (red) cyclonic eddies. Repeat sampling stations not shown.



Hammerschmidt, 2011 and Lamborg et al., 2012 (Fig. 6). For at sea analysis of volatile gaseous Hg species (DMHg & Hg⁰), samples are immediately sparged with N₂ after CTD collection. Evading Hg is collected onto inline column traps (Tenax- DMHg, Gold – Hg⁰) that are subsequently pyrolyzed into a Tekran® model 2500 cold-vapor atomic fluorescence spectrophotometer. Peaks are measured against standardized QA/QC methods. Method Detection Limit was 11 fM. Analysis of THg followed techniques described by Gill & Fitzgerald, 1987 and modified EPA Method 1631 and Horvat et al. 1993, while MMHg analysis followed modified techniques described in EPA method 1630 and Munson *et al.*, 2014. Post-sparging transfer (A) and storage acidification (B) of sample for later analysis. Shoreside lab chemistry of MMHg (C) via pH reduction with H₂SO₄ and volatilization by NaB(Et)₄ onto Tenax columns, with similar analysis to Fig. 6 (D).

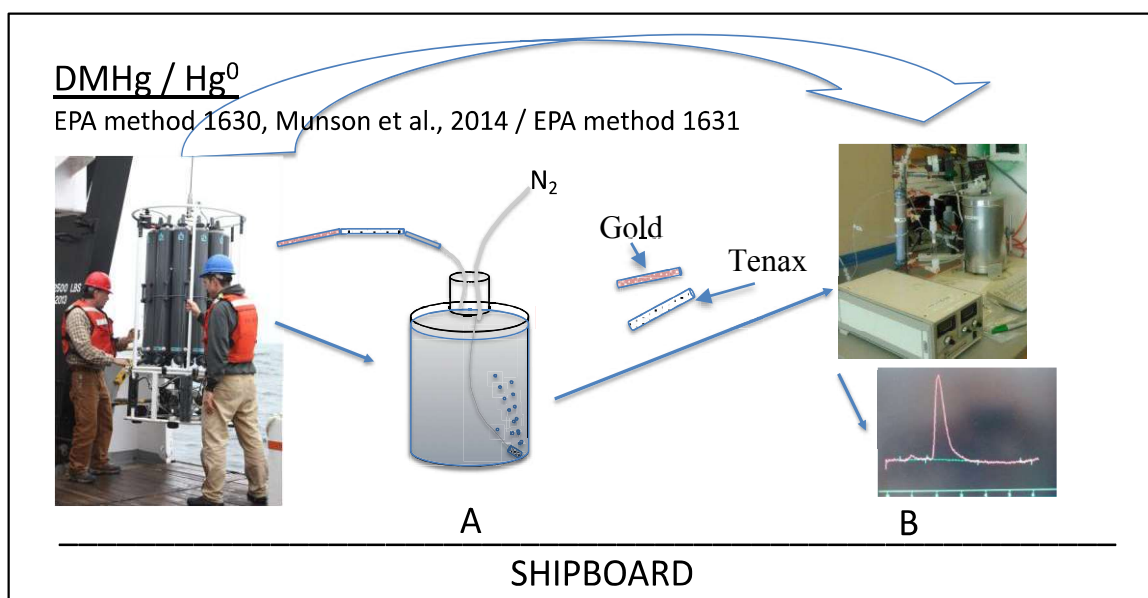


Figure 5. At sea analysis of volatile gaseous Hg species (DMHg & Hg⁰)

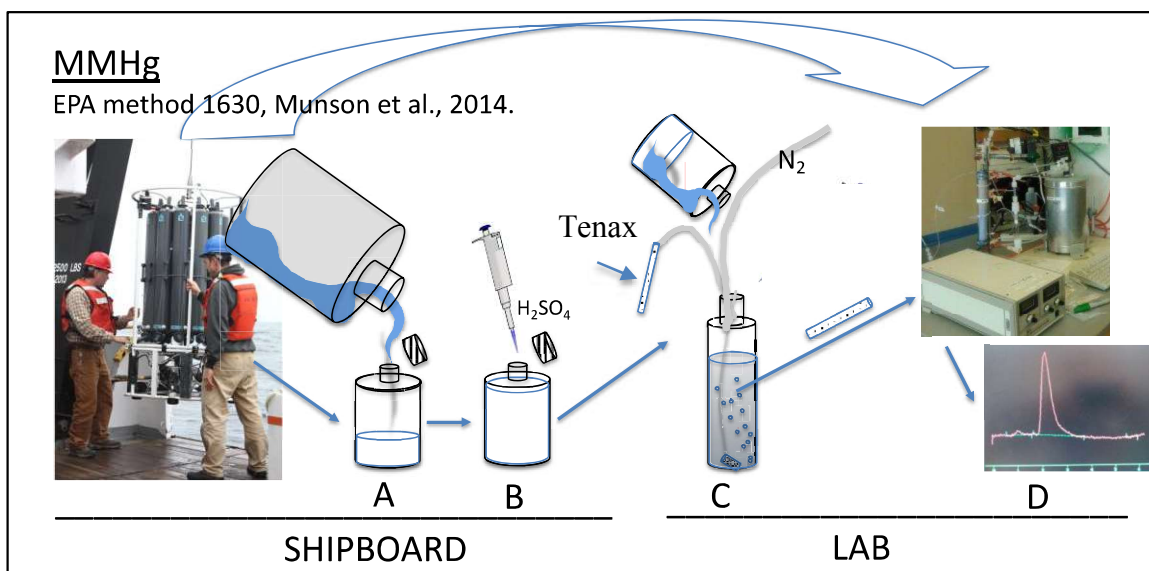


Figure 6. At sea and shoreside analysis of MMHg

Fog

To further characterize fog MMHg concentrations in relation to coastal microenvironments, fog samples were collected according to Weiss-Pienzas *et al.*, 2012, using a modified active strand cloudwater collector based on the Caltech Active Strand Cloudwater Collector (CASCC) design (Demoz *et al.*, 1996). For shipboard fog sampling, the collector was mounted on a 6-meter tower at the bow (R/V *Point Sur*), or atop the wheelhouse in a configuration that would avoid contamination from stack gasses, rigging and bow-wake sea spray (R/V *Sproul*, R/V *Oceanus*). If wind direction was not favorable for uncontaminated sampling, the sampling fan was not turned on. The CASCC was acid washed and rinsed with MQ water between samples and kept closed between collections. Prior to collection, blanks were taken by spraying 5% HCl, then MQ water into the opening of the CASCC, and 250 mL of blank rinse water was collected. Fog samples (THg & MMHg) were analyzed as freshwater using modified methods described above (preserved to 0.5% HCl).

Sediments

To investigate if shelf sediments were a significant source of methylated mercury, replicate sediment cores were taken using a multicore device (MC 800 & MC 400 Multicore, Ocean Instruments, San Diego) that preserved the sediment/water interface. Only sealed and intact cores were incubated in a refrigerator at bottom water temperature for two days, before the overlying water was analyzed for mercury species. Replicate cores were sectioned then had porewaters extracted via centrifugation prior to analysis of mercury species. The upper few centimeters of undisturbed cores were sectioned at the following depth increments: 0.5, 1, 1.5, 2, 3, 4, 5 cm. Porewaters were extracted via centrifugation and the MMHg gradients were used to calculate fluxes into the overlying water column based upon molecular diffusion alone. For the fluxes listed below, we used the formula:

$$F_D = -(\phi D_w / \theta^2) / (\delta C / \delta x)$$

where ϕ is the sediment porosity, θ is the tortuosity, D_w is the, molecular diffusivity coefficient of $5 \times 10^{-6} \text{ cm}^2 \text{ sec}^{-1}$, C is the concentration of MMHg in pore water, x is the sediment depth (Choe *et al.*, 2004). The value of θ^2 can be estimated from porosity using the relationship $\theta^2 = 1 - \ln(\phi^2)$ (Boudreau, 1996). Sediment solid phase, pore waters and overlying waters incubated onboard were analyzed for MMHg and THg.

Neuston & Sea Surface Microlayer

To resolve and constrain any potential fluxes at the air-sea interface during 2014 cruises, the upper 10-1000um of sea surface or SML (Sea Surface Microlayer) were sampled in with an acid cleaned 2L polycarbonate bottle. This method was exploratory and meant to detect large enrichments despite dilution. Assuming a 10 μm SML thickness (Wurl & Obbard, 2004), and idealized sample collection at the diameter of the polycarbonate bottle, a dilution factor was calculated (Fig. 8). This dilution factor was applied to these surface grab samples post-analysis to estimate the expected theoretical concentration of MMHg at the air-sea boundary layer.

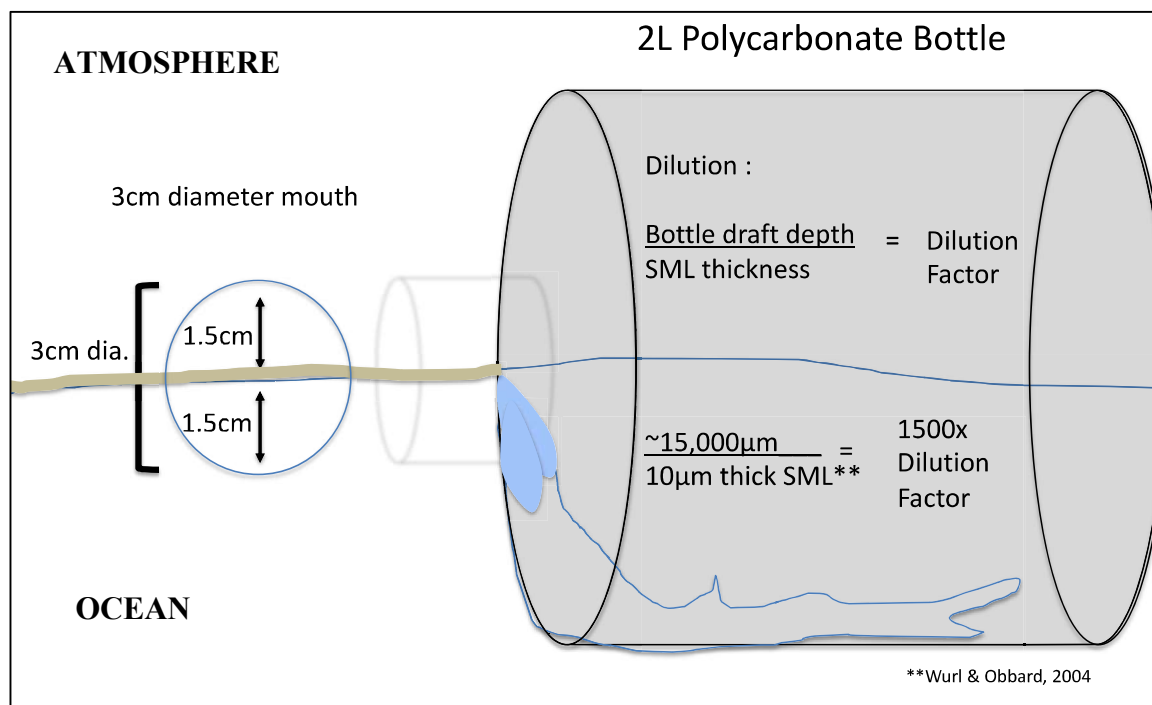


Figure 7. SML sampling, targeting the air-sea interface and dilution factor calculations.

RESULTS & DISCUSSION

Vertical Profiles

THg and Hg^0 concentrations were typically 1000x larger than methylated species (MMHg & DMHg). Shallow shelf profiles (30-100m) of all mercury species measured were generally well mixed with no substantial gradients, likely due to dynamic circulation of water over the shelf environment, as well as coarse sampling (Fig.9 & 10). Deeper (~1000) offshore profiles of THg and Hg^0 gently increased with depth (Figure 11). Methylated species indicate a sharp surface mixed layer depletion, with concentrations slowly increasing with depth (Fig 12 & 13), prompting a few potential explanations.

MMHg complexing with dissolved organic compounds, its adsorption onto particles, and phytoplankton uptake, all subject to removal from the mixed layer via the biological pump, could influence this pattern (Hammerschmidt and Bowman, 2012;

Lamborg *et al.*, 2016). Photodemethylation and photodegradation within the photic zone may also play a role in surface water MMHg depletion (DiMento & Mason, 2017).

DMHg, as a volatile gaseous species, likely degasses and evades into the atmosphere.

Both species have the potential to influence fog concentrations through the air-sea boundary. DMHg fate and pathways within this coastal zone of study is discussed later in Chapter 3.

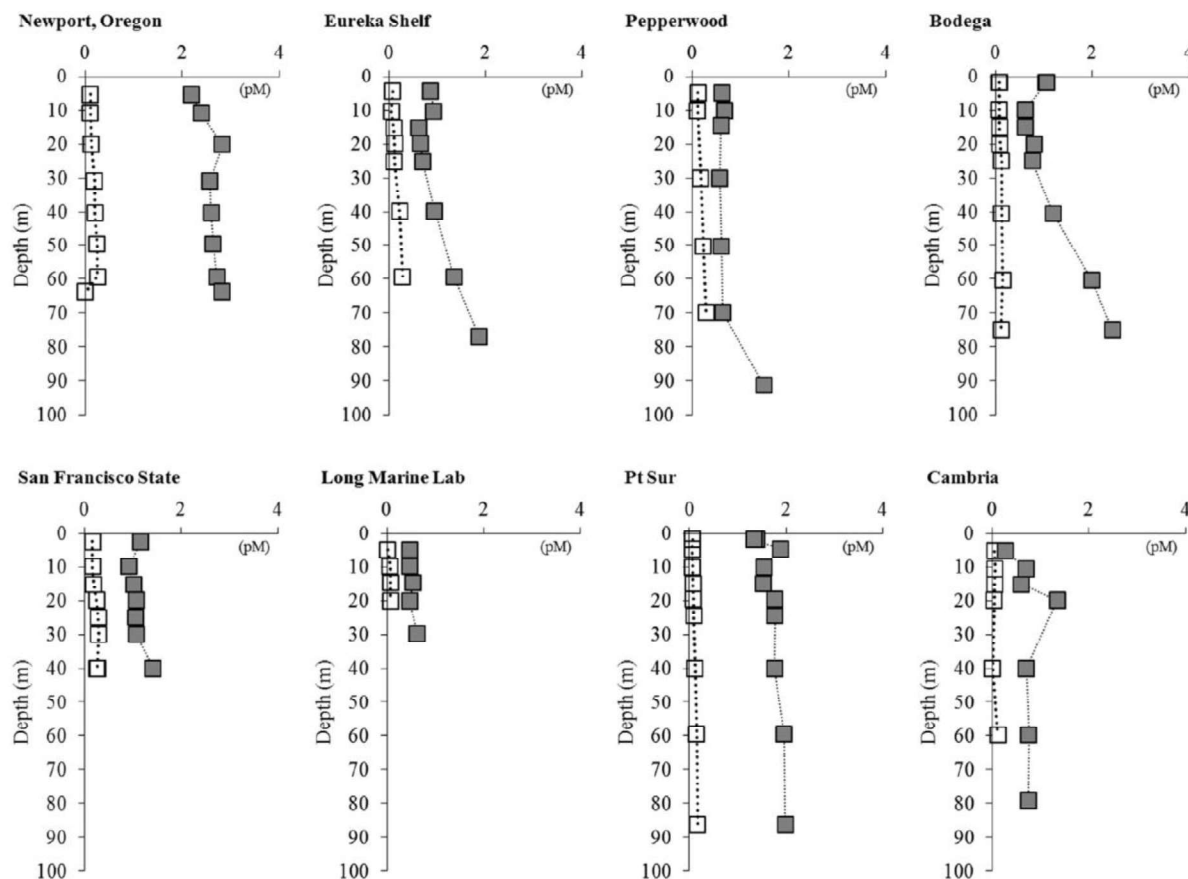


Figure 8. Mercury species distributions in the water column overlying shelf sediments. Vertical profiles for Hg^0 (open squares) and THg (filled squares) from selected stations showing characteristic trends for these species.

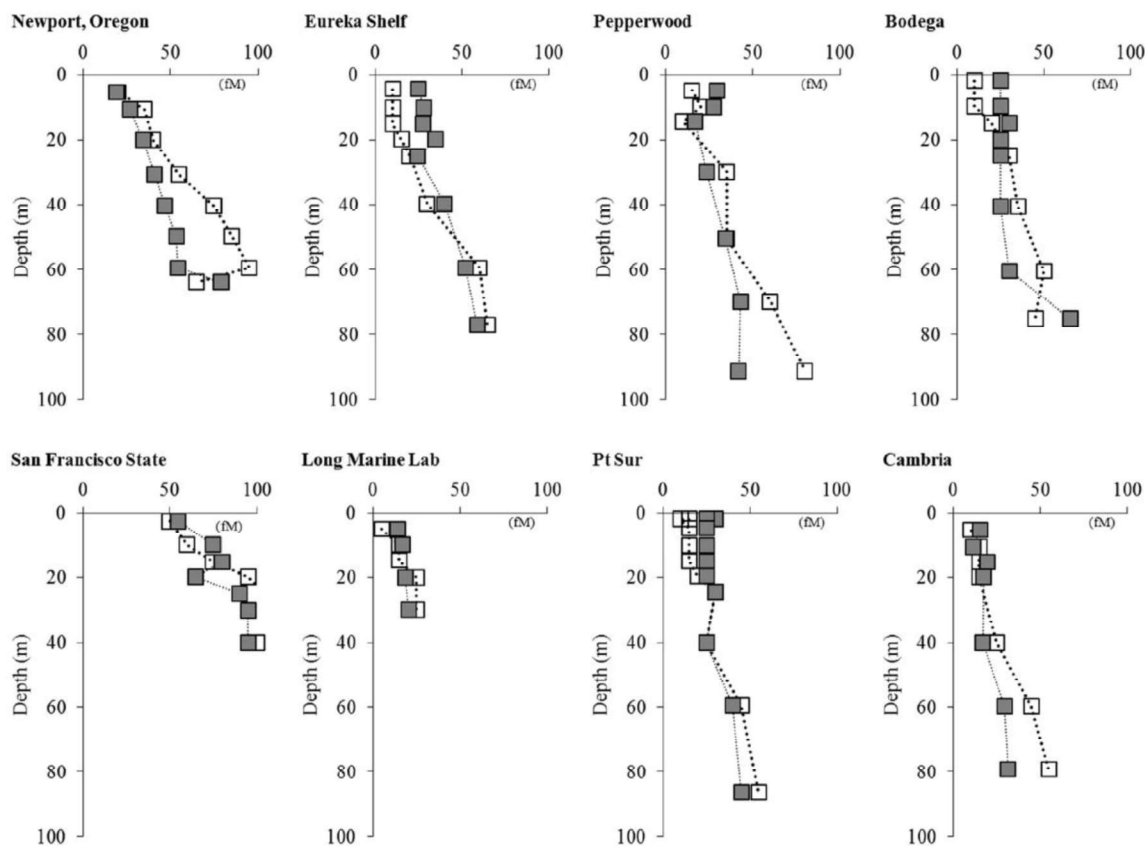


Figure 9. Methylated mercury species distributions (fM) in the water column overlying shelf sediments. Vertical profiles for DMHg (open squares) and MMHg (filled squares) from selected stations showing characteristic trends for these species.

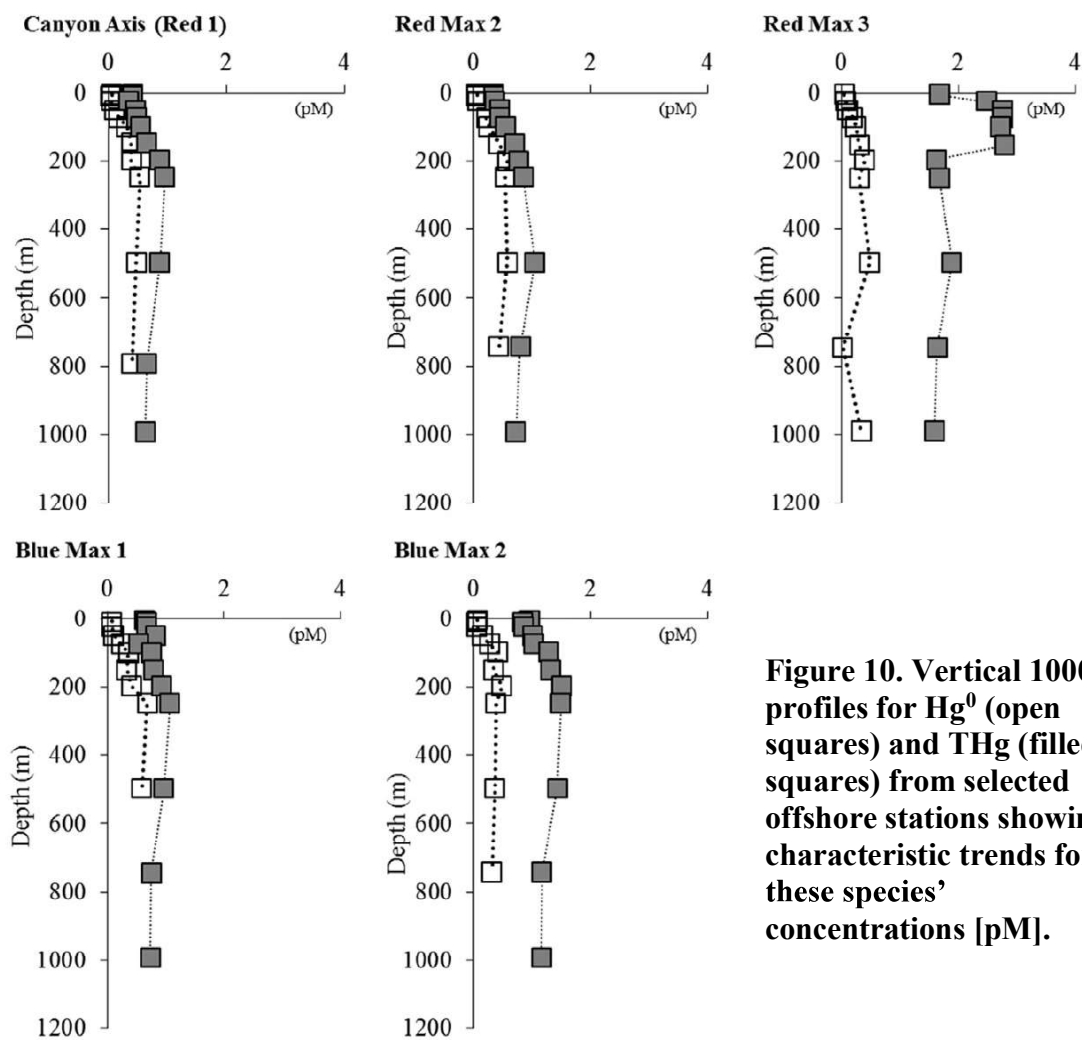


Figure 10. Vertical 1000m profiles for Hg^0 (open squares) and THg (filled squares) from selected offshore stations showing characteristic trends for these species' concentrations [pM].

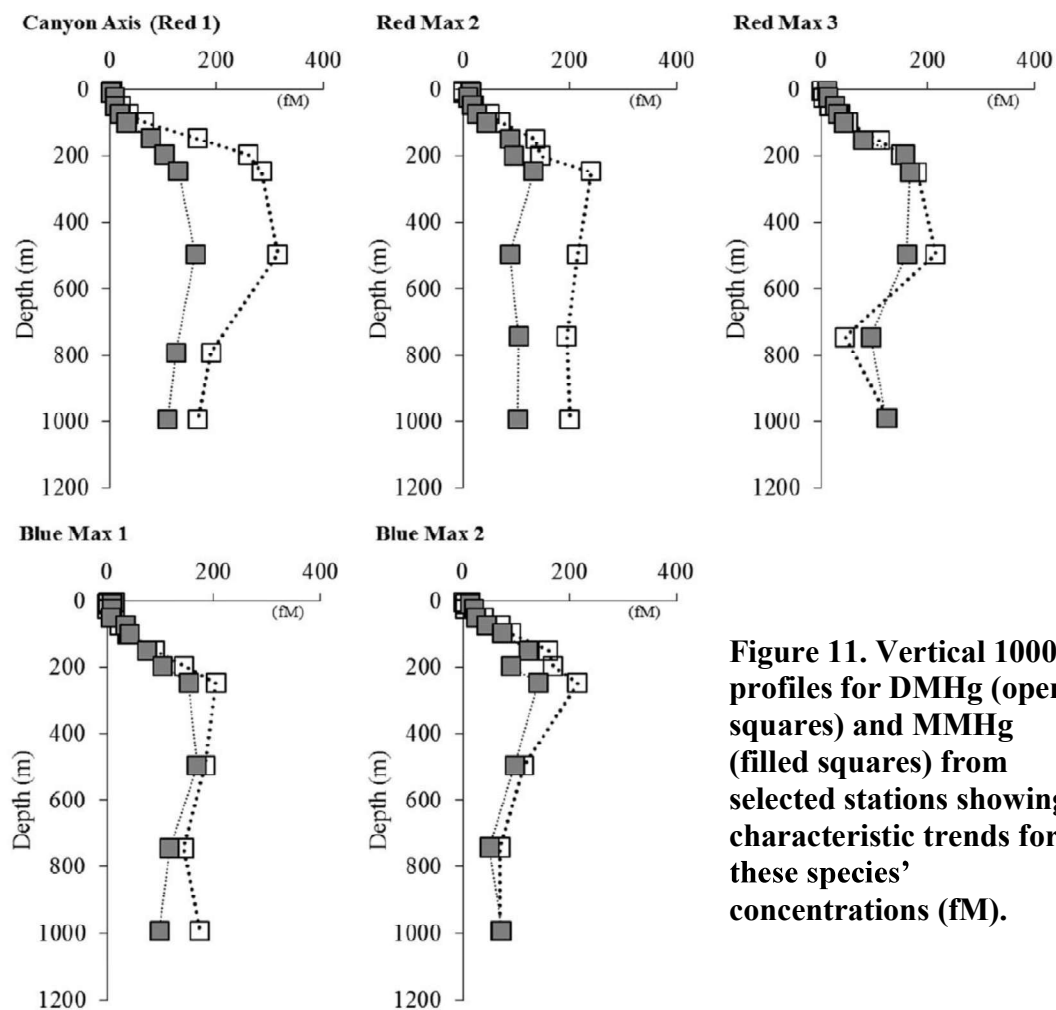


Figure 11. Vertical 1000m profiles for DMHg (open squares) and MMHg (filled squares) from selected stations showing characteristic trends for these species' concentrations (fM).

Sediments

Shelf pore waters (20-90m) were generally elevated with respect to MMHg, which resulted in benthic fluxes from 0.1-1.7 pmoles m⁻² day⁻¹ (Table 4.). However, these fluxes are ~10% of the air-sea flux at the ocean surface. Comparatively, MMHg benthic flux values from the US east coast measurements ranged from 7 – 13 pmoles m⁻² day⁻¹. (Hammerschmidt & Fitzgerald, 2006) East coast sediment production rates account for 50-80% of water column concentrations (Balcom *et al.*, 2004). These 20-fold differences are likely driven by the respective bathymetry of the coastal shelves. The shallower, broader east coast shelf environment generally receives more organic carbon, anthropogenic and riverine inputs that comprise coastal shelf sediments (Seaber *et al.*, 1987; Oczkowski *et al.*, 2016), resulting in a higher benthic flux into a smaller water column. The narrower west coast shelf appears to have a markedly smaller influence on MMHg water column concentrations.

Table 3. Sediment-water diffusive flux estimates for continental shelf stations.

Station	MMHg Pore water pM	MMHg Benthic flux pmoles m ⁻² day ⁻¹
Ventura	0.140	0.1
Conception	0.473	0.4
Cambria	1.018	0.7
Long Marine Lab	1.660	1.2
Shelter Cove	0.738	0.5
Port Orford	0.360	0.3
Coos Bay	2.175	1.7
Florence	0.693	0.5

Sea Surface Microlayer

Surface grab sampling of the air-sea interface on the 2014 cruises has shown this layer to be slightly enriched in MMHg (Fig. 14). When calculating for dilution of the sampling method, estimated SML MMHg concentrations increased by 1500 (~10pM) (Fig. 15), an enrichment orders of magnitude higher than most trace metals in the SML (Table 2). This suggests higher than expected exposure implications for organisms and

materials (microplastics) inhabiting this micro-environment (See Chapter 2). Yet the surface grab methodology was not the most accurate available, thus requiring a refocus of effort targeting the microlayer. With a finer resolution we can adequately confirm these preliminary results.

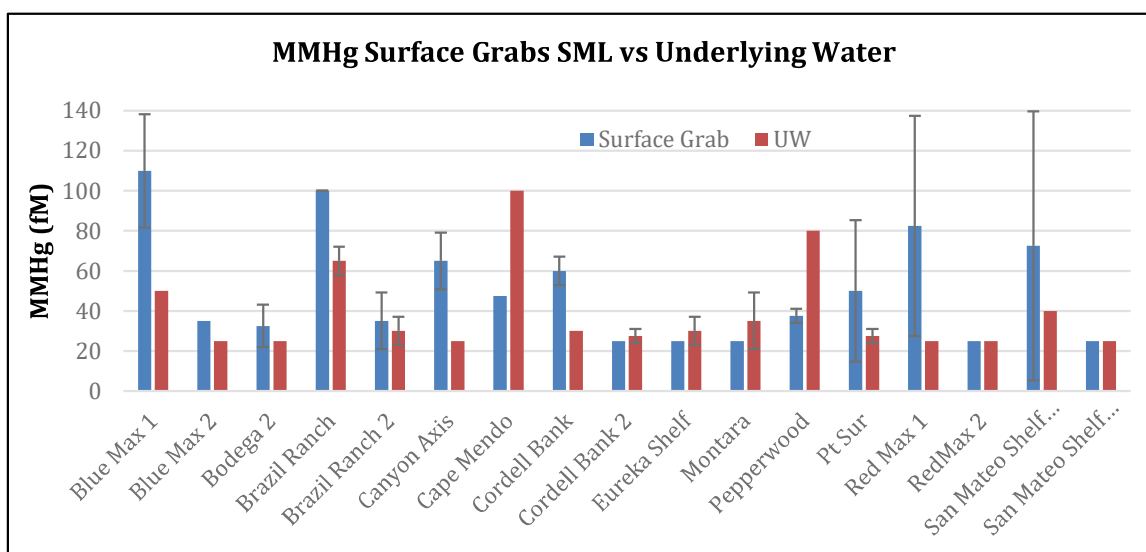


Figure 12. Diluted (uncorrected) surface grab MMHg SML and underlying water (UW) samples taken during a series of California Current cruises described in Coale *et al.*, (2018).

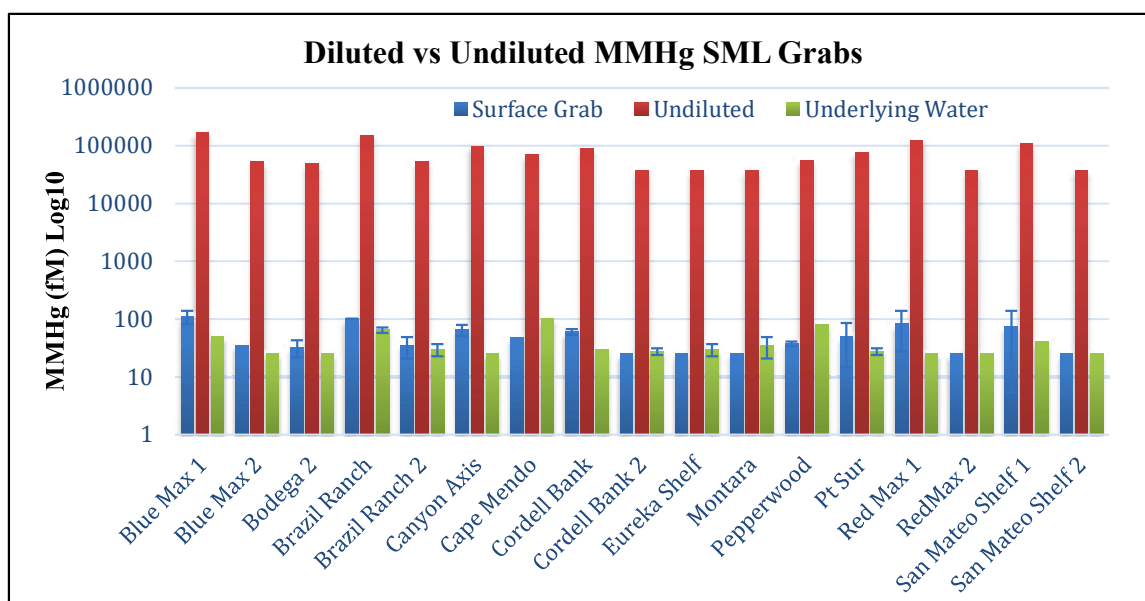


Figure 13. Diluted (uncorrected) surface grab samples shown relative to undiluted (corrected) SML MMHg estimated concentrations (*fM*).

Chapter 2

The Sea Surface Microlayer (SML)

Surface films and slicks at the ocean's surface have been observed and queried as far back as Aristotle; however, only recently have they been understood with the advent of new technology and analytical techniques (Aristotle, No.38; Franklin & Brownrigg, 1774; Rayleigh, 1890; Pockles, 1891; Langmuir, 1917; Langmuir, 1938; Ewing, 1950). While conceptualized earlier, Sieburth (1983) was the first to propose the SML as a thin (~10-100 μ m) slick or film composed of gel-like hydrophobic organic material present at the air-sea boundary. Planktonic organisms such as diatoms contribute proteins and carbohydrates and lipids that form a significant portion of the SML (Fig. 16, Engel *et al.*, 2017; Cunliffe & Murrel, 2009; Galgani & Engel, 2013). SML environments are unique in that they are the interface for chemical, biological and physical processes, as well as a dominant feature for buoyant life forms such as fish eggs and larvae. The accumulation

of nutrients and contaminants at the SML yields high concentrations of these constituents (Wurl & Obbard, 2004).

A mercury (Hg) and MMHg enriched SML may represent a source of MMHg to coastal marine fog. It is from this layer where ocean wave and foam generated bubbles are ejected into the atmosphere as sea spray aerosols (SSA), often becoming cloud condensation nuclei (CCN) (Fuentes *et al.*, 2010; Prather *et al.*, 2013; Garbe *et al.*, 2014). SSA are one of the largest natural contributors to global atmospheric aerosols, consisting primarily of NaCl crystals coated in sulfates, organic species, carbonates and other hygroscopic salts (Ault *et al.*, 2013). Increasing wind may increase microlayer thickness until disrupting the SML, and decrease the organic fraction of SSA material (Gantt *et al.*, 2011). Due to the lipophilic nature of MMHg, significant partitioning of MMHg from the bulk mixed layer into the SML may make it preferentially susceptible to aerosolization (Aller *et al.*, 2005). This chapter investigates the role the SML plays in the cycling of mercury species from the oceans to the terrestrial environment via fog transport and other coastal processes.

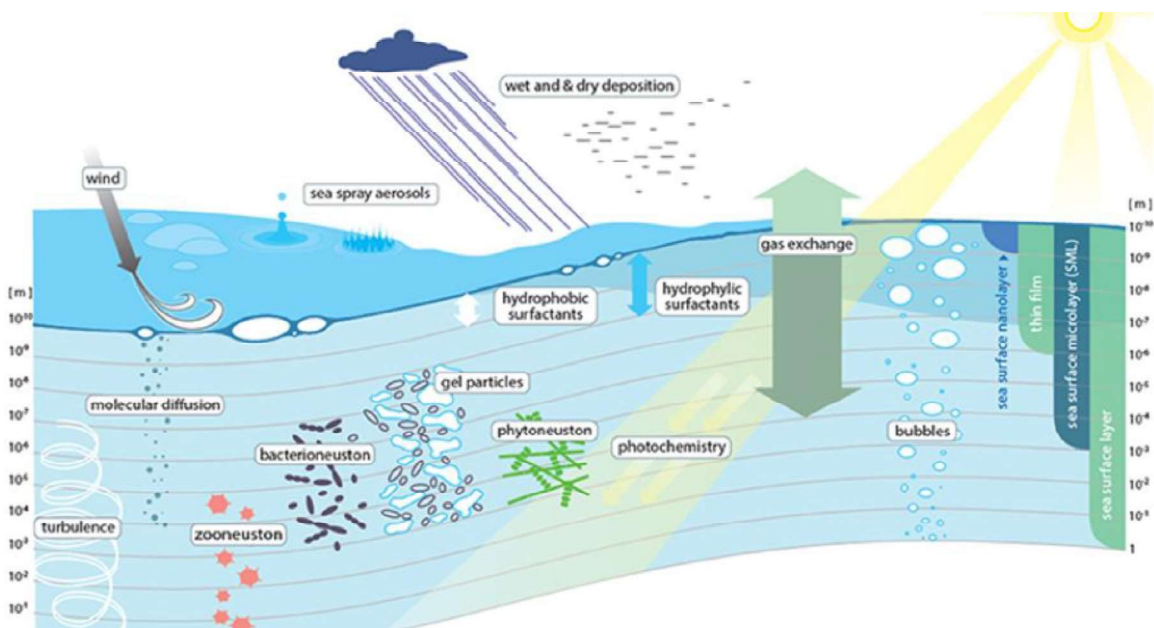


Figure 14. Conceptual model of the Sea Surface Microlayer. Engel *et al.*, 2017

Surfzone Aerosols

Fog collections spanning ~450km offshore and inland of the California – Oregon sampling region exhibit peaks in MMHg and MMHg/THg ratios at the land-sea interface (Fig. 17, Coale *et al.*, 2018), suggesting the nearshore coastal regions and or surf zone are greater potential sources of MMHg aerosol than offshore for potential marine fog uptake. Marine aerosol composition encompasses the wide range of terrestrial and marine materials that become entrained in the atmosphere (Prospero, 2002). The surf zone is responsible for generating aerosol concentrations at ~1-2 orders of magnitude greater than offshore environments (Leeuw *et al.*, 2000). The SML is an overlooked potential source of MMHg to the atmosphere and coastal fog, originating from the aerosolization of this compound via escaping gas bubbles (Gantt *et al.*, 2011).

METHODS

Study Site

34 ocean sampling sites sampled during the summer of 2015 extended from Ventura, California to Newport, Oregon (Fig. 18) aboard research vessels *R/V Robert Gordon Sproul* (June) and *R/V Oceanus* (August). As a part of Chapter 1, these cruises are the same that focused on measuring marine compartments (water column, sediments, neuston and mesoscale surface anomalies). From 2016-2018, SML and surface water sampling was conducted locally within Monterey Bay using small workboat platforms from Moss Landing Marine Labs (MLML). Using methods described in Chapter 1 and Coale *et al.* (2018), all THg, MMHg, and DMHg samples collected in this study observed appropriate trace metal “clean” techniques, with acid washed and or pre-certified clean collection bottles, baggies and containers.

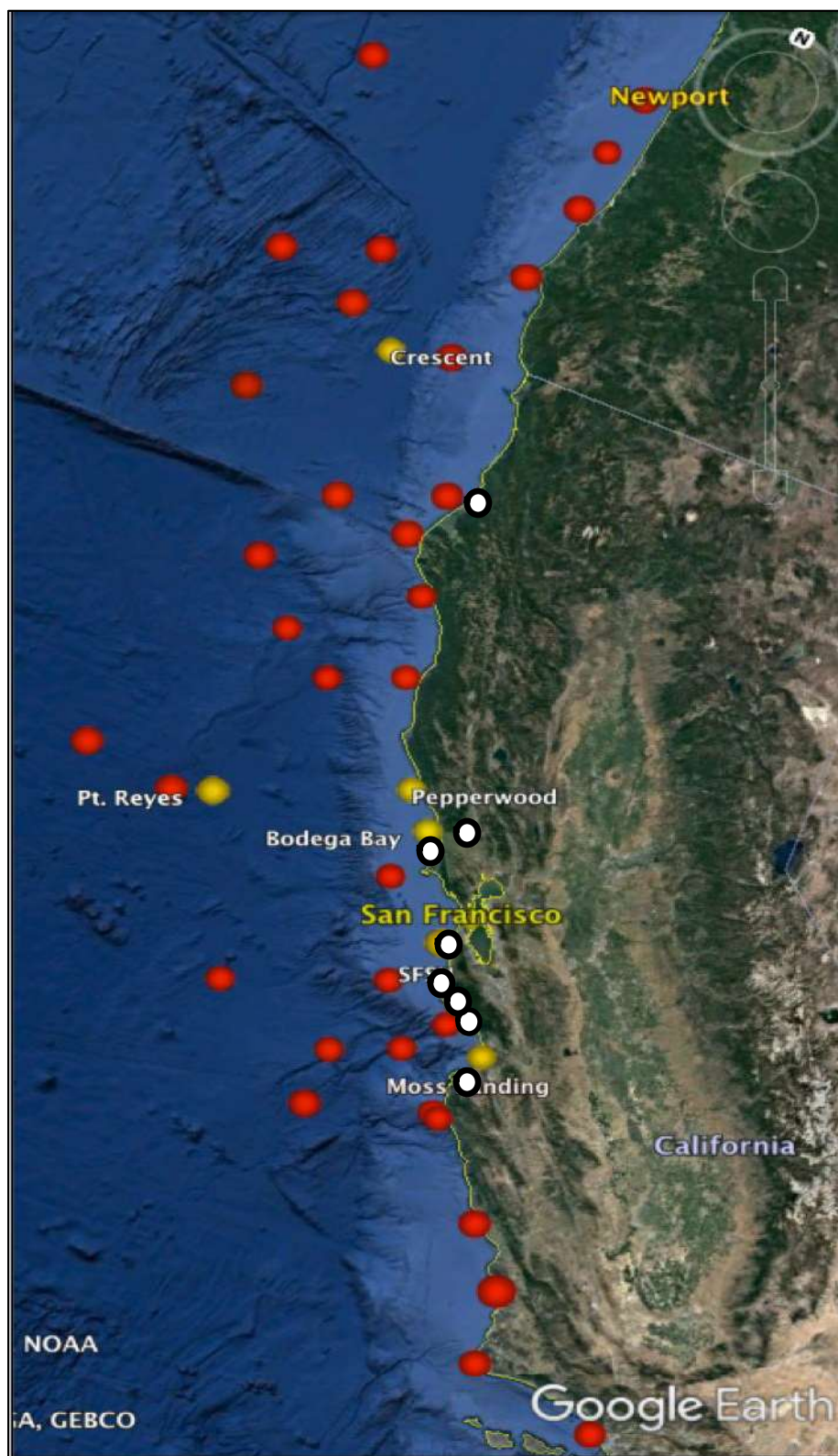


Figure 16. 2014 - 2015 cruise sampling stations (red dots), 2015 SML sampling stations (yellow dots), and *FogNet* terrestrial fog sites (white dots).

SML

In order to test the potential MMHg enrichment of the sea-surface microlayer relative to underlying water ($\sim 0.16\text{m} - 2\text{m}$ bulk mixed layer depth), samples targeting these two regions were collected during two 2015 cruises along the coastal zone between Port Hueneme, CA and Newport, OR. Subsequent sampling from 2016-2018 occurred locally within Monterey Bay, ~ 2 miles NW of Moss Landing, CA. Depending on the analyte, the SML is sampled by various operationally defined methods (Stortini *et al.*, 2012). 2015 SML samples in this thesis were collected using three glass dip sampling methods (Fig. 19), two of which are established methods in the literature:

- 1) 40 x 52 cm glass plate based on a large body of SML studies (Harvey & Burzeil, 1972)
- 2) 122 x 9 cm dia. glass tube based on Ebling & Landing, 2015
- 3) Experimental design five 122 x 3.5 cm dia. clustered glass tubes

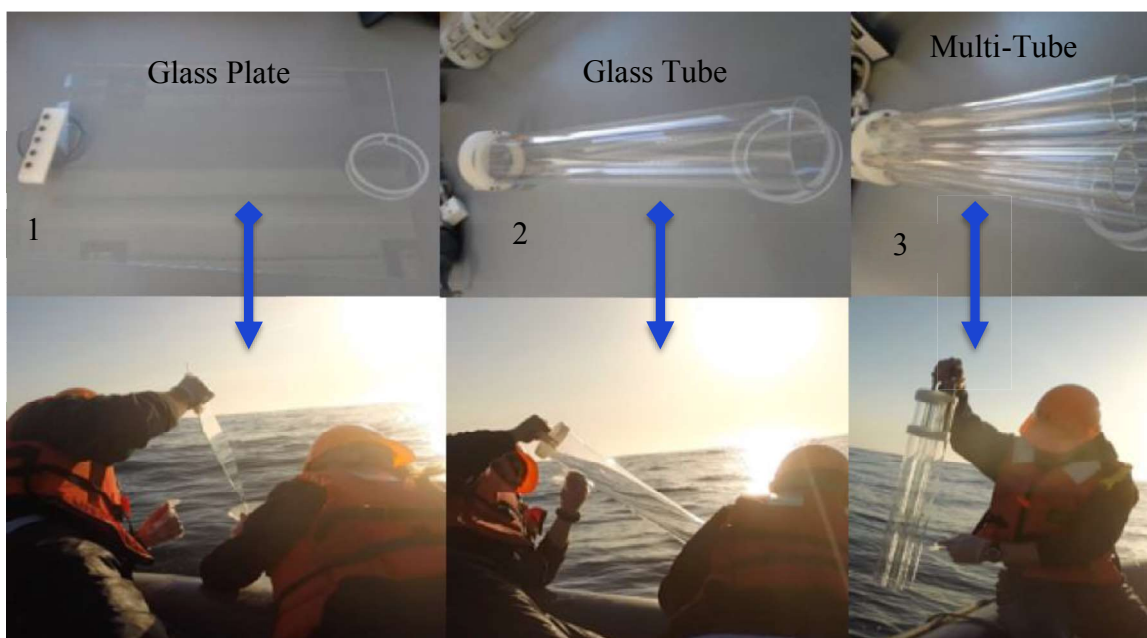


Figure 17: Glass samplers: 1) Glass Plate 2) Glass Tube 3) Glass

Prior to cruises, microlayer sampling glass plates and tubes were washed in 1% Micro® solution, rinsed with DI water, and then rinsed thoroughly in 10% hydrochloric acid (HCl). Glass was then rinsed with MilliQ filtered water and bagged.

When sea state allowed (Beaufort scale ≤ 2 : *4-7 kts, 0.5m wave height*), a small workboat/inflatable was deployed upwind of the ship to avoid any potential sea spray or exhaust from the larger vessel. Prior to targeted SML collection, glass samplers were dipped upwind of the work boat to minimize contamination, condition glass surface to ambient underlying water and rinse residual HCl from at-sea cleaning. Glass samplers were dipped as smoothly as possible into the water to within ~ 10 cm of the handle, retracted similarly and drained into a 250mL glass bottle using a plastic funnel. A silicon squeegee was used to scrape water and any material from the plate into the glass bottle. After sampling glass equipment and funnels were rinsed thoroughly with 5% HCl and MilliQ to prepare for the next sampling station. SML enrichment indexes were calculated as:

$$\text{MMHg}_{\text{SML}} / \text{MMHg}_{\text{UW}} = \text{MMHg Enrichment Factor}$$

$$\text{THg}_{\text{SML}} / \text{THg}_{\text{UW}} = \text{THg Enrichment Factor}$$

where MMHg_{SML} and THg_{SML} is the concentration of MMHg and THg in the SML, and were compared to underlying water (MMHg_{UW} and THg_{UW}). UW samples were collected using CTD rosette Niskin bottles (~ 2 m) when at sea and by hand (0.3m) from a workboat locally in Monterey Bay. A more comprehensive intercomparison between glass sampling methods was conducted after insufficient at-sea collections.

Aerosol Generator & Sea Spray

To measure and compare potential MMHg concentrations of aerosolized SML material to other coastal compartments, a novel aerosol generator was constructed. A 2”(5.08cm) PVC pipe frame and foam pontoons (Fig. 20) created aerosols within a polycarbonate dome via air bubbles entrained by water jets. A 3600gph (gallons per hour) pond pump sprayed underlying seawater out of a 1” (2.54cm) PVC pipe manifold with $\frac{1}{4}$ in (0.635cm) holes spaced 10 cm along the manifold and directed downwards. This created a series of jets that would entrain air bubbles and subsequently burst within the dome. Above the polycarbonate dome, a box attachment holding a large 203 x 264mm

glass fiber filter (Membrane Solutions) was connected to a vacuum fan, generating airflow onto the filter. The filter box was held flush over an opening in the dome to maximize flow. The aerosol generator was side-towed windward by a small whaler deployed locally from MLML and offshore (~5-8 km) in conditions less than or equal to a Beaufort Scale 2 to minimize chances of filter dilution by surface wind waves and swell. The filter box and vacuum components were also used to collect SSA from shore to compare to generated aerosols (Fig. 21).

Filter samples were collected, frozen immediately and processed in a large walk in freezer within 90 days. Approximately 1/2 - 1/3 of exposed filter area was soaked in ~250mL 0.2% H₂SO₄ solution for extraction to be analyzed after at least 48hrs. Analyses used modified techniques described in Hammerschmidt & Fitzgerald, 2006 and Hammerschmidt & Bowman, 2012. Extraction solutions were analyzed on a Tekran® model 2500 cold-vapor atomic fluorescence spectrophotometer as seawater. Roughly 1/4 of the exposed filter area was soaked in MQ to be analyzed for Cl⁻.

Ion Chromatography

Major anion concentrations for SML, fog, aerosol filter and sea spray filter samples were determined via ion chromatography with suppression conductivity detection and 29mM KOH eluent, using Cl⁻, SO₄²⁻, NO₃, and NO₂ ion standards (Coale *et al.*, 2018). While the chloride ion is not as accurate of a sea salt tracer as the sodium ion and degrades with increased atmospheric residence time, most samples were freshly collected within 1- 12hrs (Laskin *et al.*, 2012).

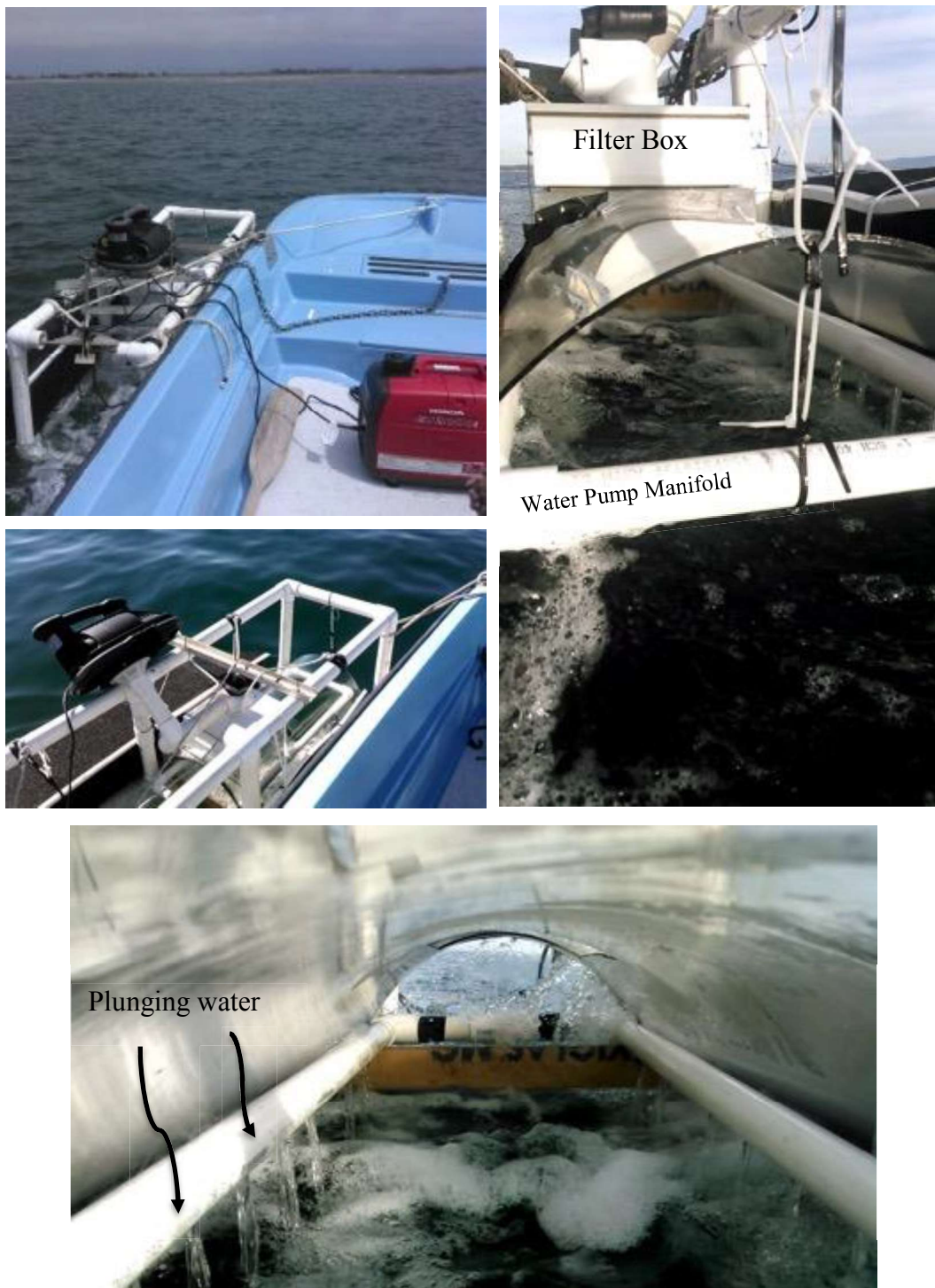


Figure 18. Aerosol generator in side-tow sampling configuration



Figure 19. Aerosol collection module (used in aerosol generator) configured for sea spray collection.

Chlorophyll

To test for the influence of Chl a on SML MMHg concentrations, Chl a in SML and UW samples were collected locally in Monterey Bay in February 2018 via aforementioned SML sampling methodology. Chl a SML and UW sample analysis followed modified methods from Welschmeyer, 1994. SML and UW samples were vacuum pump filtered through 0.7um GFF filters until filtration slowed to near-zero or the entire sample was used. Filters were then folded and inserted into centrifuge vials with 1.2mL of 90% acetone. After freezing for 48hrs, samples were centrifuged (Heathrow Scientific, Gusto) at 10,000 RPM for 2 minutes. 200 μ L were transferred to a smaller vial for measurement on a handheld fluorometer (Qubit 3.0, Life Technologies) for Chl a concentration (μ g/L) with blue excitation (430-495 nm) and red (665-720 nm) emission wavelength. This provided a bulk Chl-a measurement. To measure Chl a and its degradation products as a proxy for digestion and decomposition, a High Performance Liquid Chromatography detector (HPLC; Thermoseparations Spectra, Thermo UV6000 diode array) from absorbance at 665 nm utilized Thermo Quest chromatography software. (Note: A small pilot experiment to confirm viability of frozen

Chl-a samples before filtration showed frozen Chl samples yielded 1.75 higher fluorescence values (RFUs) than unfrozen samples on the Qubit.)

Polyaromatic Hydrocarbons & Colored Dissolved Organic Material

Polyaromatic hydrocarbons (PAHs) are a natural and anthropogenic pollutant also capable of bioaccumulating in the food web and found to be enriched in the SML. Colored/Chromophoric Dissolved Organic Material (CDOM) are the optically measurable components of dissolved organic matter (DOM) in fresh and saltwater systems. Given MMHg bioaccumulation in organic tissues and materials, SML and underlying bulk water samples were analyzed to test for any potential relationship between CDOM and PAHs. After initial MMHg analysis, SML and UW samples were analyzed for PAH and CDOM using Excitation-Emission Matrix Spectroscopy (EEMs) (Johengen *et al.*, 2012).

Fluorescence intensity contours were generated from a SPEX ISA Fluoromax-2 scanning spectrofluorometer using quinine sulfate (QS) standards and MATLAB GUI for area calculations. Fluorescence spectra were over an excitation range of 230-500 nm (5 nm intervals) and an emission range of 300 – 600 nm (3 nm intervals). An integration time of 1 second was used for each scan, with bandpass widths of 5 nm for both excitation and emission spectrometers. Xenon lamp intensity and emission monochromator performance were verified and recalibrated before analysis. For all EEM's, dark counts were subtracted and spectra were corrected for wavelength-dependent instrument effects using correction files. Fluorescence spectra intensities were normalized to the area under the Raman peak using MilliQ water. EEM's of MilliQ water served as background blanks for sample EEM's. A four-point calibration curve (0-50 ppb) of Quinine Sulfate (QS) in 50 mM H₂SO₄ was run at the beginning and end of each analytical batch to track drift in fluorometer. The QS response factor standardized emission intensities across each analytical batch. All sample EEM's were corrected for Raman and Rayleigh scattering peaks.

RESULTS & DISCUSSION

SML

From the two 2015 cruises, MMHg in the SML and underlying water from the mixed layer ranged from 16.02 - 380.39 fM and 4 – 48 fM respectively, corresponding to enrichment factors (EF) of 2.5 – 29.6 (Fig. 22, Table 5). *For this particular graph, averaged GT/MT samples where GP measurements were absent* While MMHg enrichment of the SML exhibited noticeable trends with seawater temperature, fluorescence (chl proxy), PAR (sunlight) and potentially wind speed (Fig. 23), only temperature was statistically significant in a single variable linear regression ($n=9$, $r^2=0.484$, $p = 0.0374$). As a multiple regression, all four variables explained ~60% of SML enrichment, yet were highly insignificant ($n=9$, $r^2 = 0.596$, $p = 0.4860$).

While there were no statistically significant correlations between oceanographic parameters and enrichment factors, likely due to high environmental variability (Wurl *et al.*, 2004, 2011, 2017) and low sample size, there were some noticeable trends. The positive relationship between SML MMHg enrichment and temperature (Fig. 16a) may be indicative of a thicker microlayer built up by local or regional converging and downwelling water masses (Pegliasco *et al.*, 2015). However, any pattern of MMHg SML enrichment by eddy type appeared inconclusive, with more sampling needed to be certain (Fig. 24).

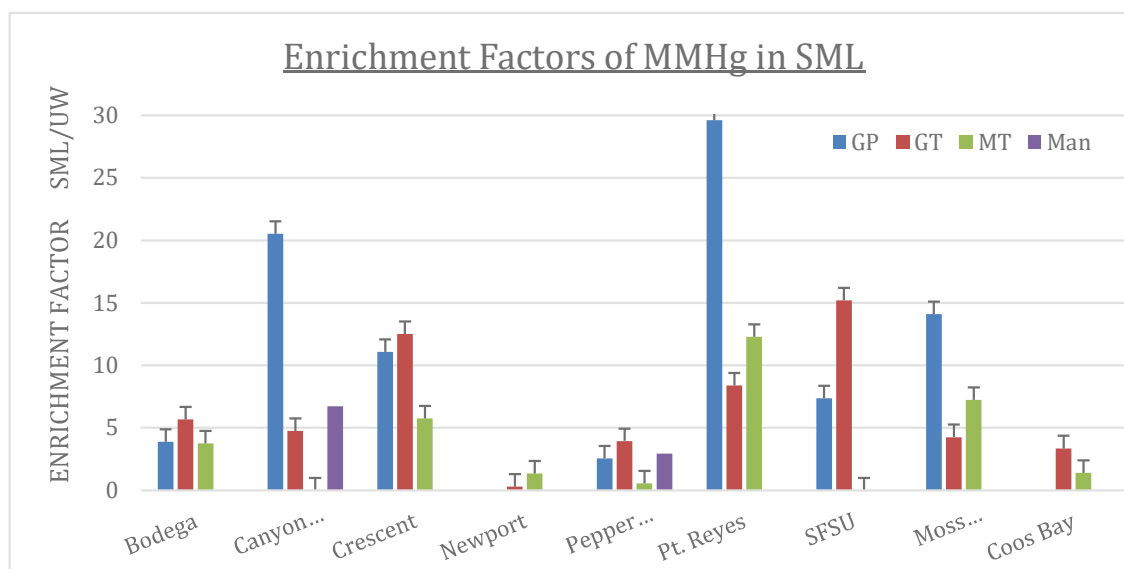


Figure 20. MMHg enrichment factors in the SML and collection method from 2015 cruise stations.

Station	EF (GP *GT/MT)	Salinity ‰	Temp C°	Oxygen μmol/Kg	Fluorescence mg/m3	Wind Spd knots	PAR μE/Sec/Meter^2
Bodega	3.88	33.77	11.05	209.37	2.88	3.4	503.72
Canyon Axis	20.52	33.18	18.6	234.04	0.16	5.29	0.45
Crescent	11.08	32.57	13.73	259.79	0.93	8.2	810.87
Newport	1.3*	30.97	12.95	304.2	1.6	3.9	677.3
Pepperwood	2.55	33.17	13.19	329.6	8.49	4.17	2.72
Pt. Reyes	29.62	33.05	15.6	259.09	0.73	10.2	84.5
SFSU	7.36	33.139	13.6	278.85	7.1	15	1821.06
Moss Landing	14.11	33.16	14.11	239.4	3.47	2	563.2
Coos Bay	3.36*	33.37	13.72	283.67	1.44	11.83	62.29

Table 4. MMHg average SML enrichment factors via glass plate collection method and paired oceanographic conditions from 2015 cruise stations. (*GT and MT averages used when GP was unable to be used)

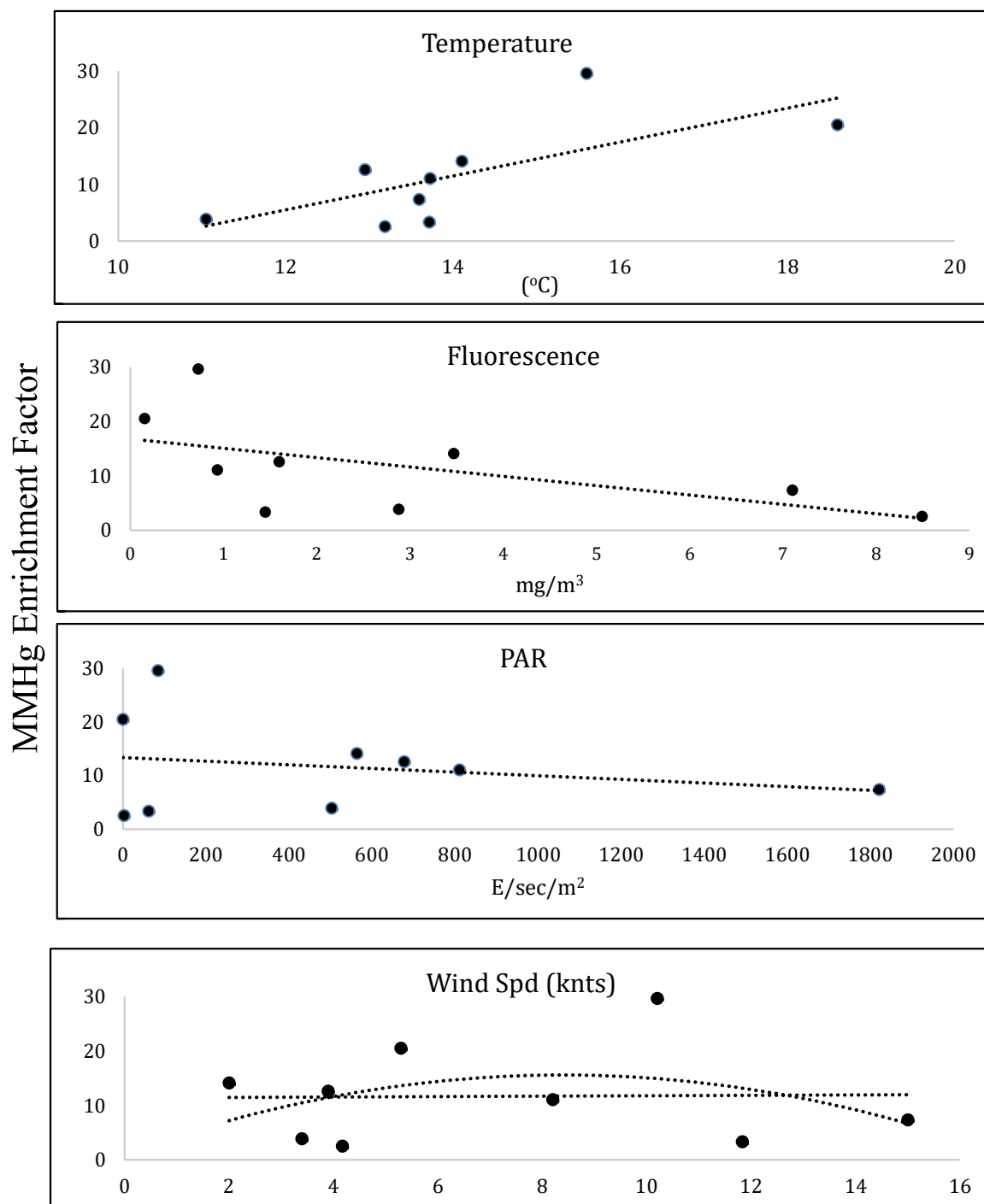


Figure 21. Notable trends between SML MMHg enrichment factors and oceanographic parameters (temperature, fluorescence, PAR, wind speed).

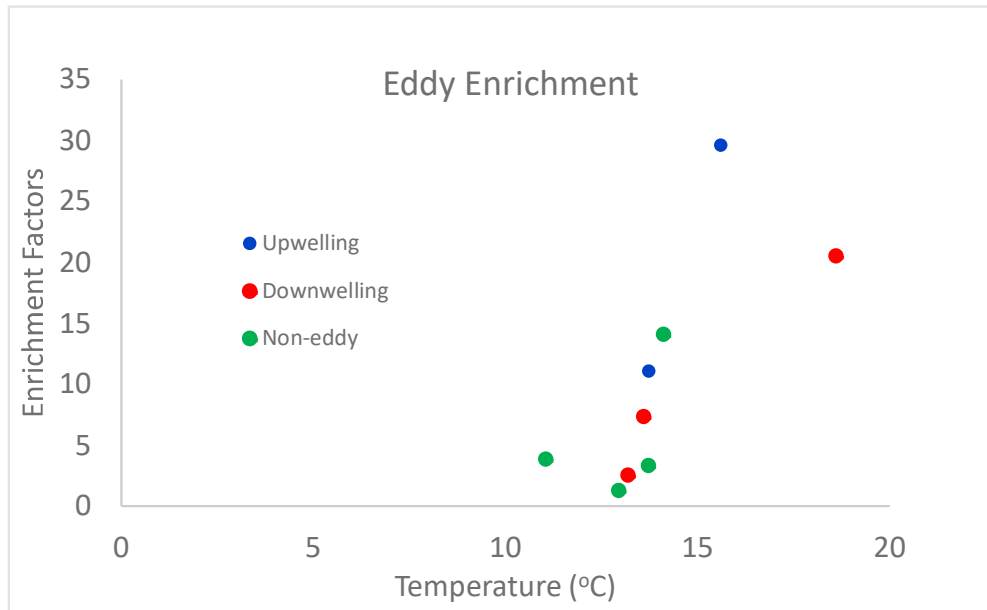


Figure 22. MMHg SML enrichment factors based on temperature and mesoscale

These salient negative trends' lack of statistical significance (SML MMHg enrichment with respect to fluorescence (chlorophyll-a proxy) and PAR (Fig. 23)) points to the integrated processes of phytoplankton growth, photodegradation and photodemethylation from related studies (Mason *et al.*, 2012; Dimento & Mason, 2017). Planktonic exudates may be the most dominant source of MMHg to the SML via the apparent passive and active uptake of MMHg by phytoplankton (Lawson & Mason, 1998; Pickhardt & Fisher, 2007; Shiuan & Fisher, 2017). Dissolved organic matter (DOM) may influence MMHg enrichment factors by regulating phytoplankton uptake (Lee & Fisher, 2017), however there were no comprehensive measurements of DOM during this sampling. Due to the nature and location of this microenvironment, is apparent that many other processes are controlling the measured variability.

SML material can thicken with increasing winds until reaching a critical speed at which wind waves and wind stress destroy and dissipate this layer (Reinthal *et al.* 2008; Kuznetsova *et al.*, 2004). MMHg SML enrichment and wind data measurements were too few to conclusively support this observed phenomenon.

Despite this variability between sampling tool and sites, an enrichment can be found across all stations and sampling tools. The 2-30x MMHg enrichment of the SML,

relative to UW, supports and refines 2014 cruise findings (Fig. 14 & 15) and are the first such measurements to our knowledge. While much less than the 1500x theoretical concentration, the results also appear to be the largest enrichment in an open ocean environment like the coastal Pacific (Table 6).

All air-sea boundary processes pass through or incorporate this region of concentrated MMHg. Floating organisms and objects such as microplastics, larvae and other neuston are exposed to MMHg and other SML pollutants, presenting potential novel pathways for MMHg bioaccumulation into marine foodwebs (Song *et al.*, 2015). Microplastics are of great concern as they contaminate the marine environment and pose a direct and indirect health hazard to organisms of various sizes when ingested (Fig. 25, Cole *et al.*, 2013; do Sul *et al.*, 2014). Microplastics are among many materials that may float at the surface and accumulate within the SML (Song *et al.*, 2014; Wurl *et al.*, 2017), thus potentially coated in MMHg-rich material provide a “pre-concentrated” exposure greater than normal surface water MMHg concentrations. The SML may be a vector of MMHg to inhabitants of and visitors to the ocean’s skin and air-sea boundary layer.

[illegible]

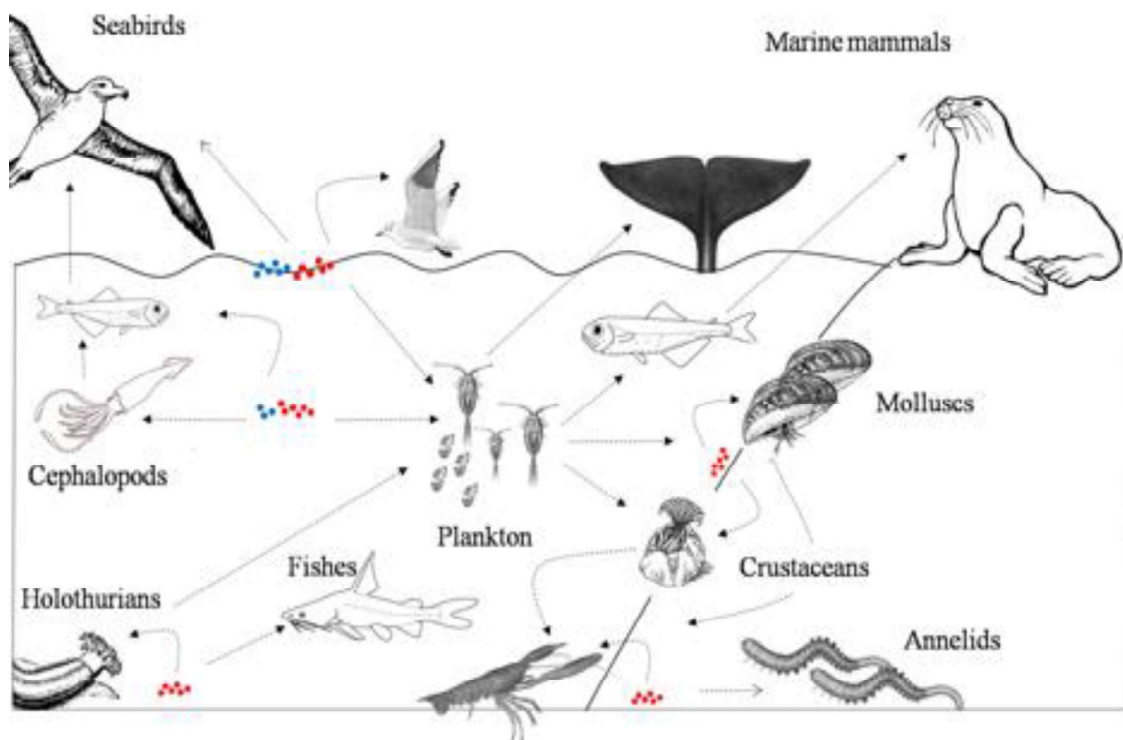


Figure 23. Microplastics ingestion pathways throughout the marine foodweb. From do Sul *et al.*, 2014

The SML enrichment values of MMHg also represent the higher end of other trace metal enrichments in this microenvironment (Table 2). The lipophilic nature of MMHg and upward transport via bubble plumes and or buoyant gel particles and aggregates likely lend to its partitioning into the accumulated hydrophobic organic material of the SML (Azetsu-Scott & Passow, 2004; Zhou *et al.*, 1998), potentially more so than most metals.

MMHg/ Cl^- ion concentrations measured across coastal compartments help characterize the marine MMHg contribution to coastal fog, utilizing the Cl^- ion as a tracer of marine origin (Fig. 26) (See *Aerosol Generator, Sea Spray & Fog*). If the SML were contributing most of the MMHg found in fog, we would expect this ratio to be much higher compared to fog, since that MMHg would mostly be associated with Cl^- ions from marine derived organic compounds. While the SML is indeed enriched with MMHg and was measured by more accurate and tested means, it does not appear to provide enough

of a source concentration to account for MMHg concentrations in fog, given the higher MMHg/Cl⁻ ratios found in fog.

Glass sampling methods are almost certainly still diluted by virtue of the sampling technique itself (i.e. dipping/penetrating into bulk UW, dip speed, handling). Despite relatively large enrichment factors, contamination from underlying water diluting the microlayer could explain why these concentrations fall short of a theoretical 1500x enrichment from the 2014 cruise surface grabs. MMHg SML enrichment is a recently heretofore unmeasured source of MMHg to the atmosphere and terrestrial ecosystems via sea spray aerosols (Weiss-Piensas *et al.*, 2016).

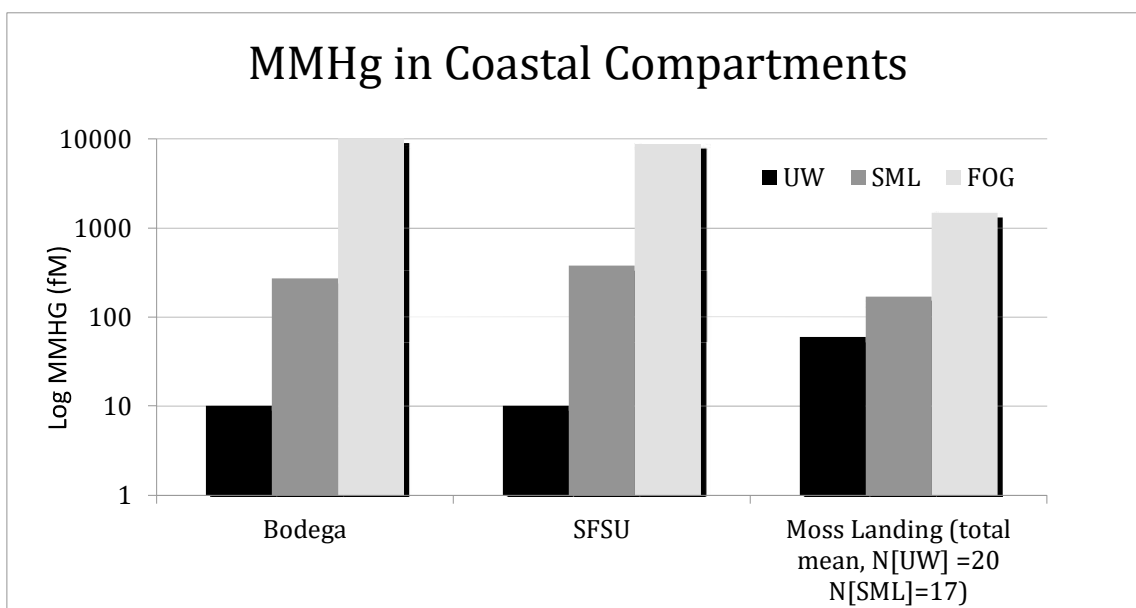


Figure 24. MMHg concentrations in coastal compartments.

SML Sampler Comparison

Based on the relatively large standard deviation for absolute SML concentrations for GT and GP methods (Fig. 27a), SML glass sampling methods varied only slightly by

enrichment factors (GT: 2.4, GP: 2.7, MT: 2.5; Fig. 27b) and sampling efficiency ($MMHg [fM] / cm^2$: GT: 0.0229 ± 0.0176 , GP: 0.0207 ± 0.0148 , MT: 0.0134 ± 0.0023).

This variability is consistent with the known composition and patchiness tendencies of the SML microenvironment, as previously suggested by Wurl & Obbard, 2004. Despite lab and field experiments showing rapid reformation of disturbed surface films (Dragcevic & Pravdic, 1981; Williams *et al.*, 1986), larger scale physical oceanographic conditions (winds, breaking waves) leading to greater dissipation and dilution likely depletes MMHg-containing material within the SML. To some extent, MMHg partitioning into phytoplankton (via passive or active uptake) and eventually zooplankton may also play a role in determining spatial and temporal distribution of MMHg within the pool of SML organic material.

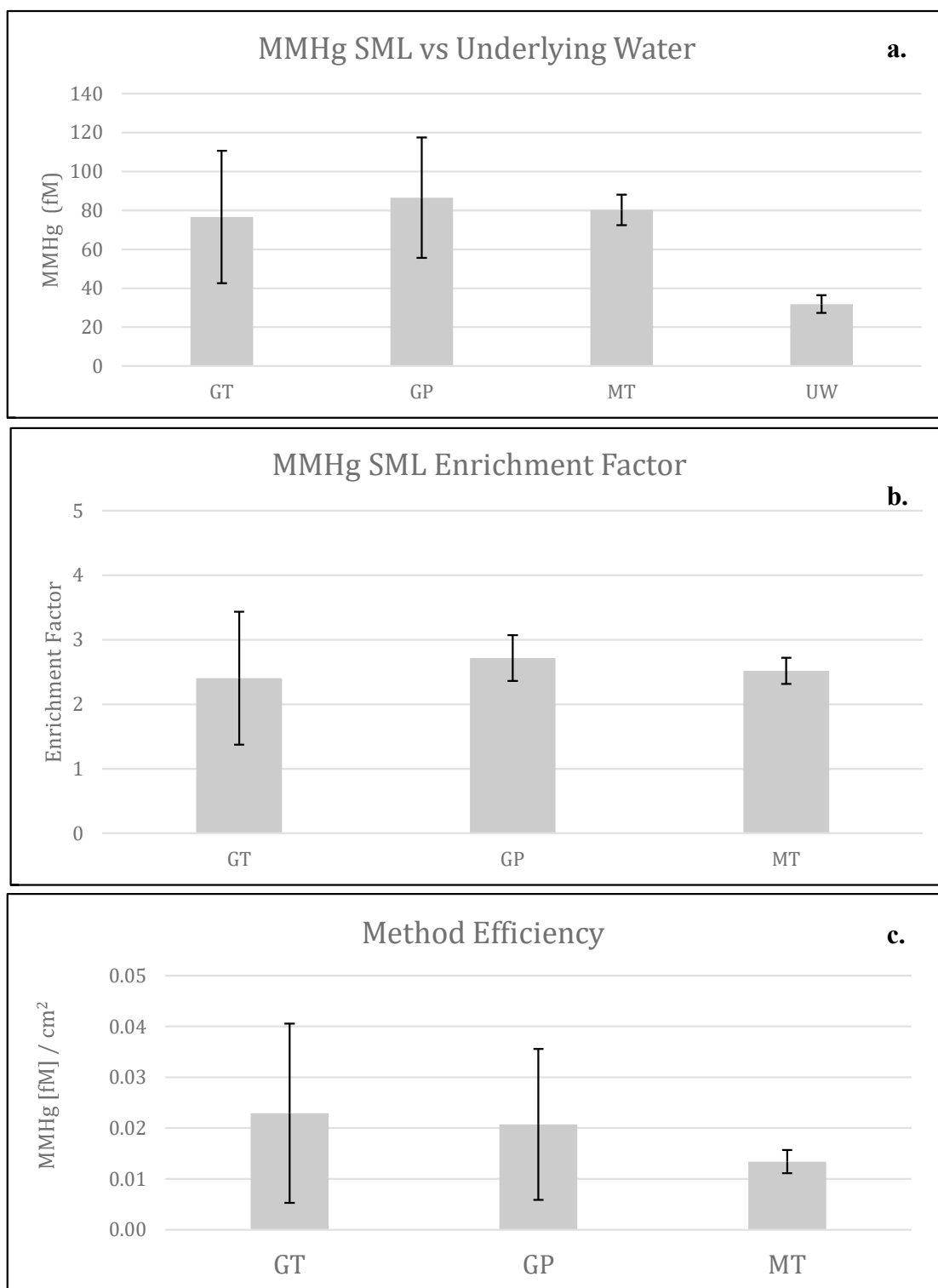


Figure 25. SML collection methods compared to a) underlying water b) MMHg SML enrichment factors and c) SML MMHg collection efficiency

THg Enrichment & MMHg Fraction

SML samples collected during February 2018 for MMHg/THg comparisons showed no noticeable enrichments ($EF > 1$) in the SML for MMHg, while THg were as high as 25 for nearshore samples (~3-5 miles) (Fig. 28, Table 7). Save for one anomalous UW sample (Fig. 29), MMHg/THg fraction as a percent in SML and UW samples were similar to those in seawater from other measurements (Bowman *et al.*, 2015; Sunderland *et al.* 2009). However, MMHg SML enrichment was nearly zero (Fig 28, while THg enrichments were mostly around 5-fold. This agreement in the MMHg fraction between SML material and seawater, and no SML enrichment may indicate a few possibilities: 1) THg enrichments are a relic of photodegraded or biodiluted MMHg, or 2) organic MMHg material is lingering just below the surface, and has not risen to accumulate in the SML (a mixed layer profile for this site would have answered this). Photodegradation and active winter weather that characterized the time of year sampled, are likely factors for these results.

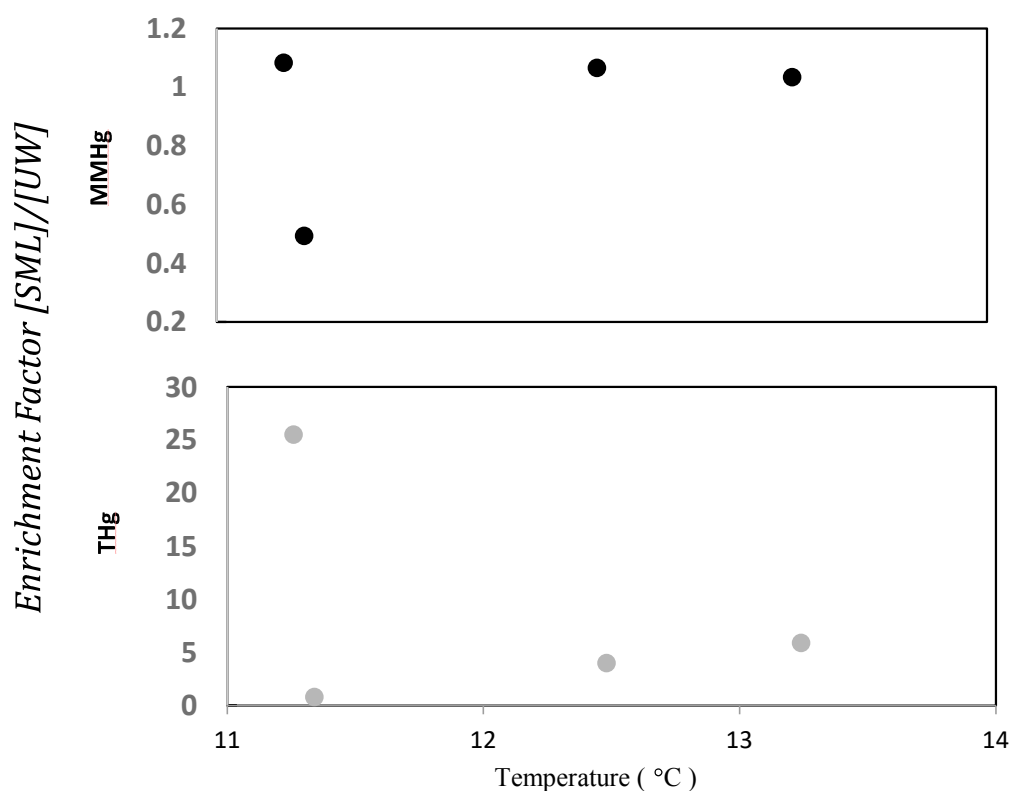


Figure 26. SML Enrichment Factors for MMHg and THg collected during February 2018.

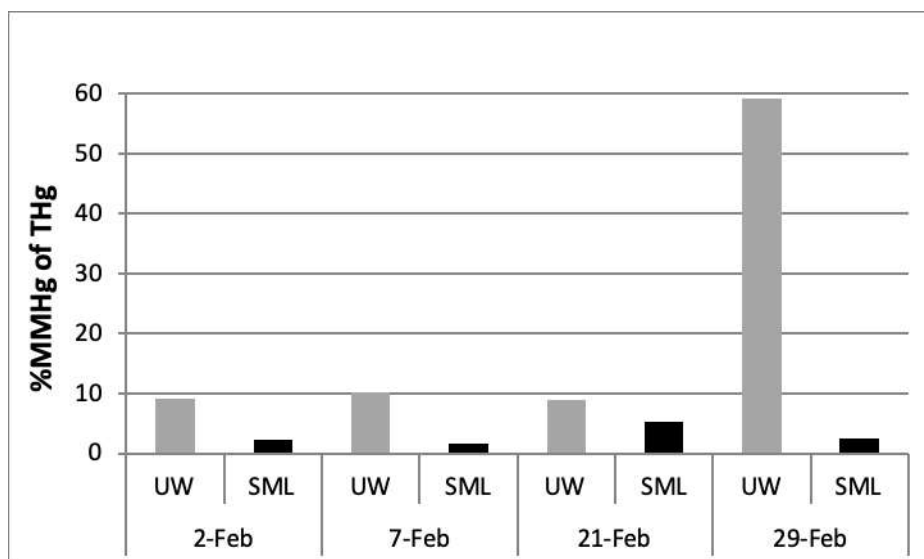


Figure 27. Percent MMHg of Total Hg in SML and UW

	THg [<i>fM</i>]				MMHg [<i>fM</i>]			
	Temp (°C)	UW	SML	EF	UW	SML	EF	Avg MMHg % THg
2-Feb-2018	12.5	1045.8	4183.3	4.0	94.8	101.1	1.1	5.7
7-Feb-2018	13.2	788.4	4663.3	5.9	79.8	82.6	1.0	5.9
21-Feb-2018	11.3	922.9	751.3	0.8	81.9	40.3	0.5	7.1
29-Feb-2018	11.3	190.1	4853.4	25.5	112.7	122.0	1.1	30.9

Table 6. Avg MMHG and THg [*fM*] for UW vs SML vs EF totals and Avg MMHg as a percent total of THg (MMHg % THg)

Aerosol Generator, Sea Spray & Fog

Ratios of MMHg concentrations and tracer Cl^- ion measurements across coastal compartments increased by orders of magnitude from UW to fog water. Mean Log ($\text{MMHg} / \text{Cl}^-$) ratios for fog (collected in CASCC, 2.274) were $\sim 300\times$ higher (in absolute $\text{MMHg} / \text{Cl}^-$) than SSA filter collections (SSA, 0.207) and SSA made during two fog events (Fog/SS, 1.86), $\sim 300\times$ higher than filter collections for Bubble Aerosol filters (0.455) (Fig. 30). SML concentrations for MMHg are orders of magnitude lower than coastal fog, and when standardized for tracer Cl^- ion values ($\text{SML MMHg}/\text{Cl}^- : 8.5 \times 10^{-4}$), account for 0.03% of MMHg/Cl^- values in marine coastal fog (Fig 26). However, the shoreward increase in MMHg/Cl^- ratios of coastal compartments indicate appreciable mechanistic concentration of MMHg into aerosols relative to SML. Synthesized aerosols from the aerosol generator (BubbleAero, Fig 30) yield $\sim 20\%$ of Fog MMHg/Cl^- ratios, while SSA collected at the beach absent fog conditions (SSA, Fig 30) exhibit $\sim 9\%$. The Fog/SS data are two averaged filter measurements made during a fog event. These values are very similar to those of the aerosol generator, yet are still $\sim 20\%$ of fog samples collected via CASCC. The aerosol generator represents an apparent non-trivial source of MMHg to fog and land via sea spray, and is a proxy for SSA collected at the shoreline hundreds of meters inshore. Yet these shoreline SSA samples appear to contain less than half of the MMHg/Cl^- in the generator's aerosols. Filter measurements may be underestimating MMHg/Cl^- compared to bottled water samples, despite the effort to standardize both measurement types. Filters contain less physical volume for collection and are more prone to material saturation compared to a 250mL bottle. The fog events during which Fog/SS samples were collected on filters may also not be an accurate representation of fog events where 250mL bottled samples were collected. No 250mL fog samples were collected in tandem with filters. Sampling and analytical techniques represent some of the most current methods for in situ marine aerosol sampling generation in the lab. Higher aerosol sample sizes across a variety of conditions may elucidate this potential for MMHg concentration via aerosolization. Moss Landing salinity measurements (YSI handheld pH meter) showed normal/expected SML & UW values ($\sim 33\%$) relative to any freshwater plume from nearby Elkhorn Slough, yet Cl^- ion measurements via IC were much lower (3.2 – 6%) despite accounting for sample dilution

during ion chromatography analysis (Supplemental?). Potential over-dilution of samples aside, dynamics of SSA formation and organic SML material from jet (~500um particles) and film (~100 um particles) drops could be controlling the amount of organic MMHg-laden material collected onto sampling filters. Larger jet drops, which represent more of the UW fraction and make up a larger portion of SSA, have been shown to carry lower concentrations of organic SML material than smaller film drops (Wang *et al.*, 2017). Field experiments confirm larger particles make up most of the total SSA mass, and preferentially transfer more of their adsorbed constituents into the atmosphere (Aller *et al.*, 2017). These larger particles are also preferentially formed as marine fog particles (Sasakawa & Ooki, 2003), further restricting any potential SML film drop material containing MMHg from becoming entrained in coastal fog measured in this study

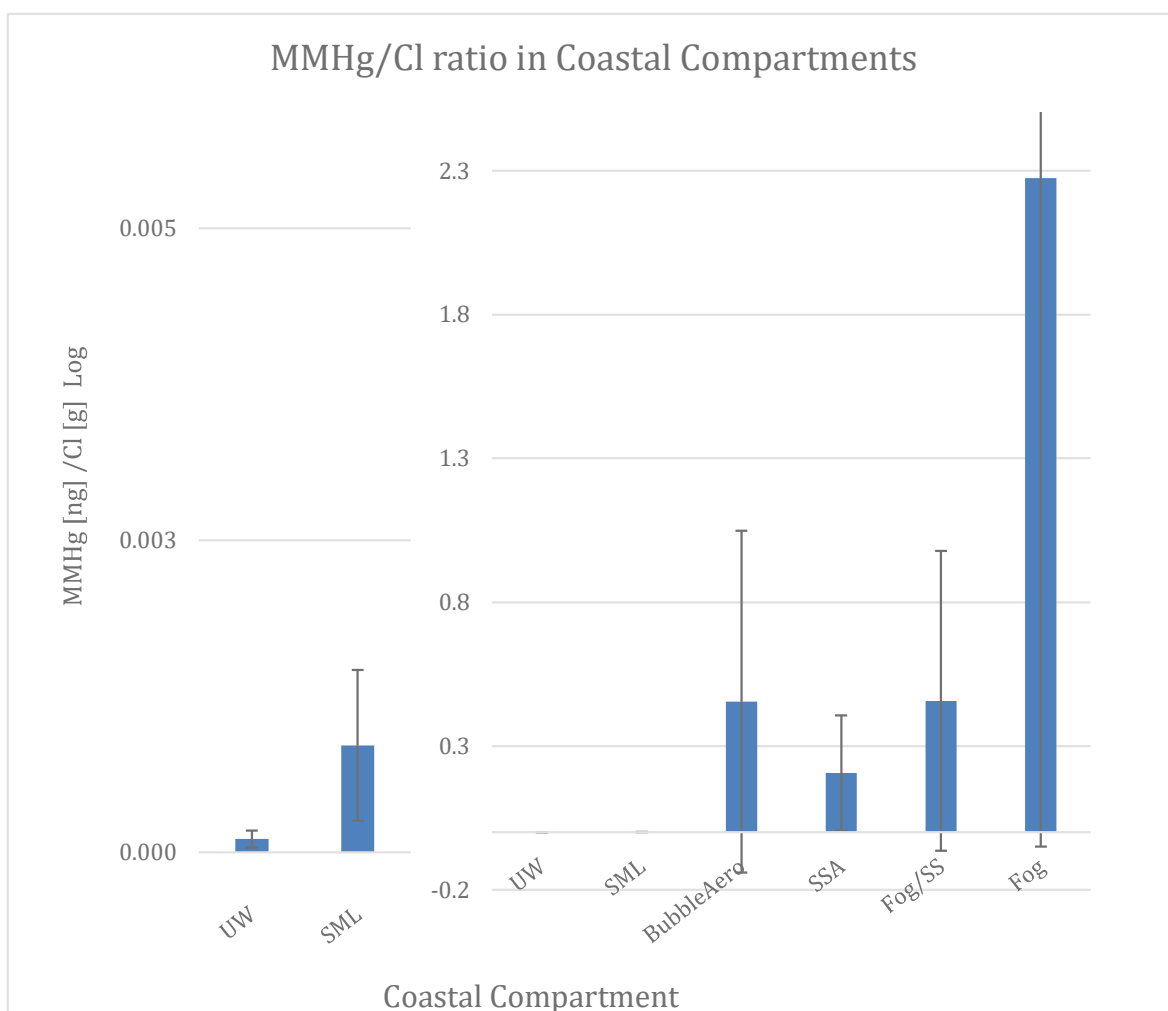


Figure 28. Potential MMHg transport across measured coastal compartments, via mean Log (MMHg / Cl⁻) ratios.

SML Chlorophyll

The lack of MMHg SML enrichment also reflected in corresponding Chl-a SML measurements (Fig. 31). Chl-a enrichment in the SML was nonexistent, with a $\sim 2.7\times$ higher chlorophyll signal in UW than the SML. Higher water temperature was associated with lower Chl-a concentrations (Fig. 31). There appeared to be no clear relationship between Chl-a and its degraded phaeopigments with MMHg in these samples (Fig. 32). Chl-a and organic material are generally enriched in the SML (Williams *et al.*, 1986; Hardy & Apts, 1989; Wurl *et al.*, 2017), however the <1 EF found in the Feb 2018 samples suggest Chl-a is likely also subject to SML variables such as patchiness, diurnal production shifts, delayed blooming, and photodegradation (Galgani *et al.*, 2014; Carlson *et al.*, 1982.). Phaeopigment abundances did not appear to influence MMHg concentrations (Fig. 32), but remains an interesting topic to revisit with higher sample sizes across productive seasons, given specific phytoplankton species may also affect SML Chl-a and phaeopigment (and thus potentially MMHg) concentrations and enrichment (Lee & Fischer, 2017; Zäncker *et al.*, 2017).

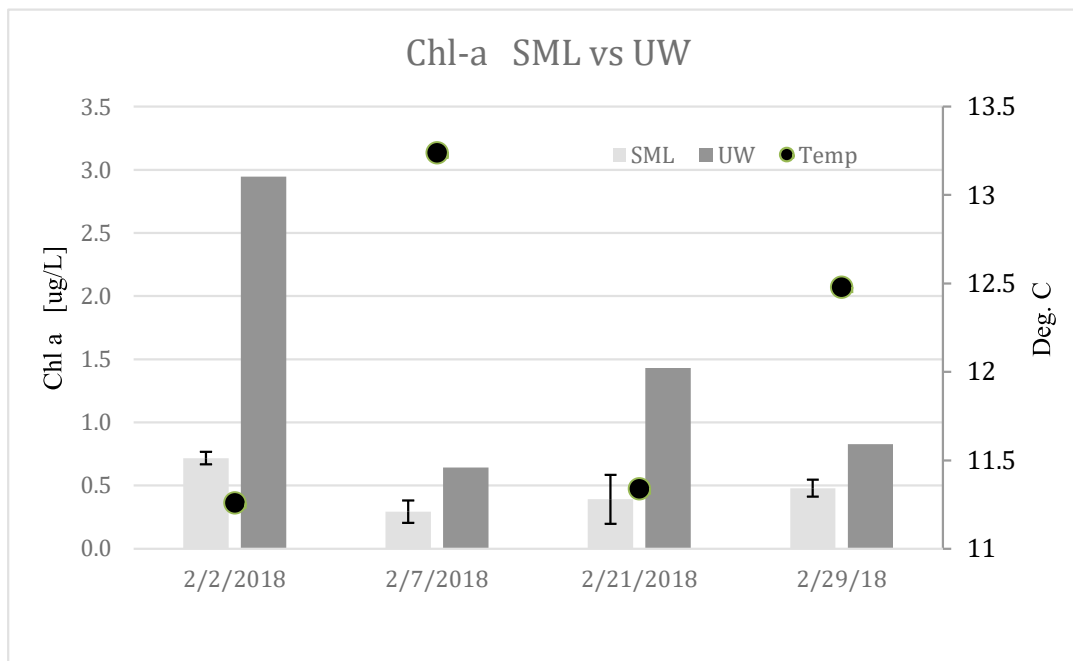


Figure 29. Chl-a [µg/L] in the SML and UW.

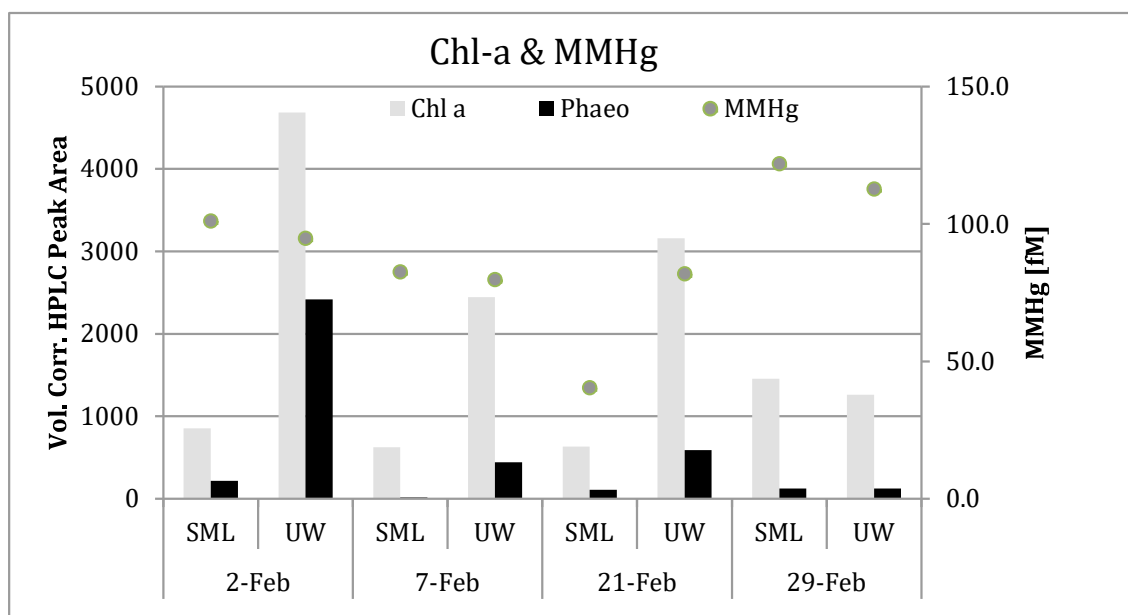


Figure 30. Chl-a and Phaeopigment fractions with MMHg [fM] in the SML and UW.

SML PAH/CDOM

Wet atmospheric deposition of PAHs can contribute significant enrichments of more than 300x to the SML (Lim *et al.*, 2007) since many PAH sources are combustion emissions (Abdel-Shafy & Mansour, 2016). While MMHg in the SML did not appear to have any relationship with PAH (a potential SML proxy) concentrations, it decreased with increasing CDOM concentrations (Fig. 33). The lack of rainfall before or during sampling of the SML could explain the lack of agreement between MMHg and PAH in the SML, considering rainfall's ability to effectively scrub the atmosphere, and MMHg concentrations elevated in marine cloud droplets at altitude relative to continental stratus (Weiss-Pienzas *et al.*, 2018). Future measurements before and after rainfall events, as well as in and out of area of high shipping traffic and industry could resolve any atmospheric flux of MMHg to the ocean and SML or lower atmospheric marine boundary layer. However, given the independent nature between PAH and marine MMHg source functions, a finding of no correlation is unsurprising.

CDOM can be formed via the microbial processing of organic matter, typically phytoplankton exudates (Thorton, 2014; Kinsey *et al.*, 2018) and are susceptible to reduced refractivity and detection under photodegradation (Miranda *et al.*, 2018). SML

MMHg trended negatively with increased CDOM fluorescence intensity (Fig. 33). SML MMHg trended negatively under increased PAR, surface temperatures and fluorescence, suggesting integrated effects of photodegradation, photoreduction (Amyot *et al.*, 1997; Lee *et al.*, 2018) and biodilution (increased fluorescence with increased productivity resulting in a diluted MMHg signal). In addition to the variability of this microenvironment, no seawater or SML samples in this study were filtered, suggesting that increased particulate matter could be influencing the amount of CDOM signal in these samples. Phaeopigments, DOM, POM (particulate organic matter) were not measured for these samples, therefore future comprehensive sampling during a more productive time of year could explain higher CDOM and lower Chl-a in this study. Sampling may have also occurred at some intermediate stage of degradation before microbial processes have fully digested the material to become optimally fluorescent. However, it seems more likely that the SML did not fully develop during sampling as a result of active wind conditions and time of year.

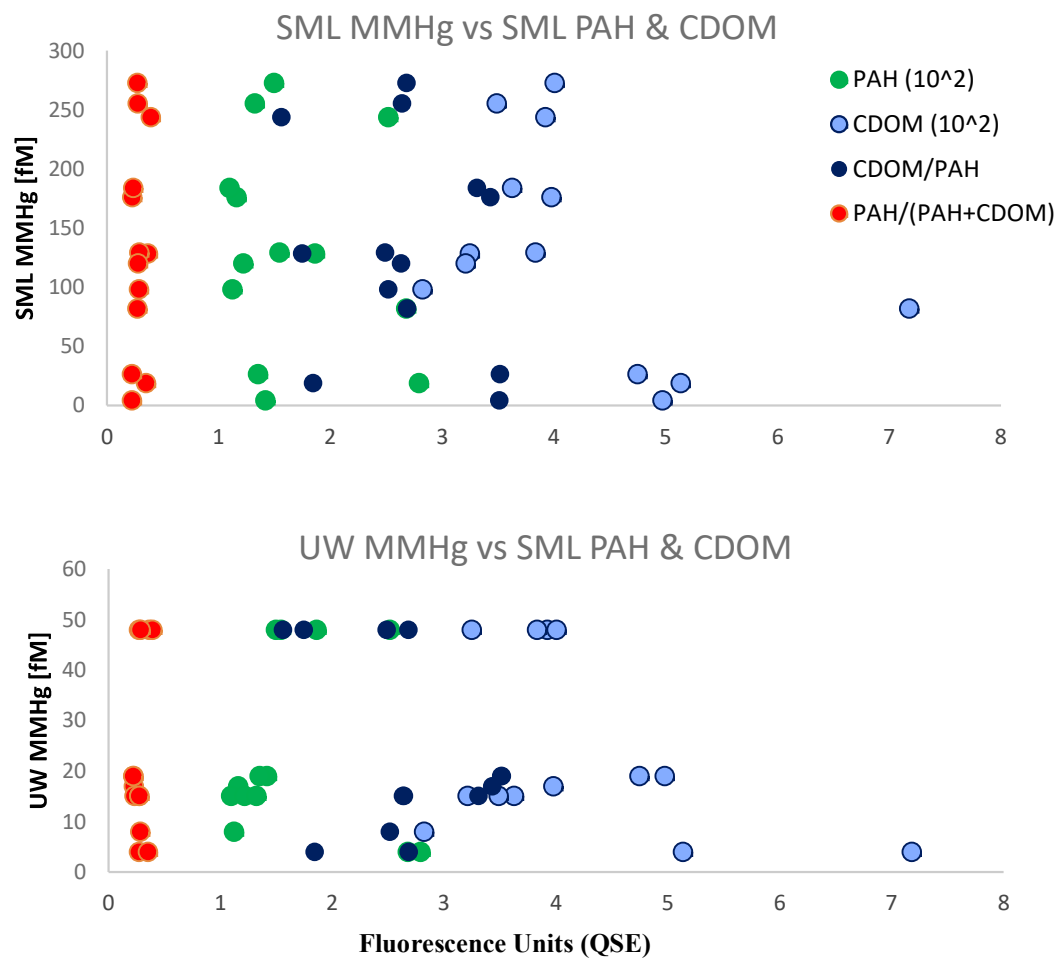


Figure 31. SML and UW MMHg compared to PAH and CDOM concentrations (Quinine Sulfate Equivalence Units, QSE).

Chapter 3

DMHg Contribution to Fog via Acidolysis

The apparent small contribution of SML and SSA particulate MMHg to marine coastal fog reflected by measured MMHg/Cl⁻ ratios suggests other marine sources of MMHg to the coastal zone that eventually becoming entrained in marine coastal fog. The coastal zone is a complex and dynamic environment that connects land and sea. Coastal California marine sources of MMHg/DMHg appear to originate from *in-situ* water column processes (~300-100m) (Coale *et al.*, 2018). Bottom water fluxes on a broader, shallow continental shelf may contribute more significantly to the levels of methylated species observed there.

Some evidence points to atmospheric DMHg cleavage as a likely source of MMHg signals within California marine fog. One of the few studies of DMHg in the upper water column in coastal California saw surface water values in the spring between 0.03 and 0.3 pM (Conaway *et al.*, 2009), showing the first clear and reproducible profiles of DMHg in the coastal Monterey Bay with surface water depletions (<0.03 pM [30fM]) and a mid-depth increase (0.6 pM [600fM]) (Fig. 34). It was theorized that surface water DMHg may evade into the lower atmosphere, transforming into MMHg and potentially recycled to the ocean or land as aerosol or fog deposition (Conaway *et al.*, 2009). While no substantiating measurements were reported in the Conaway study, this possibility has been supported by the recent findings of high levels of MMHg in fog (Weiss-Penzias *et al.*, 2012, 2016).

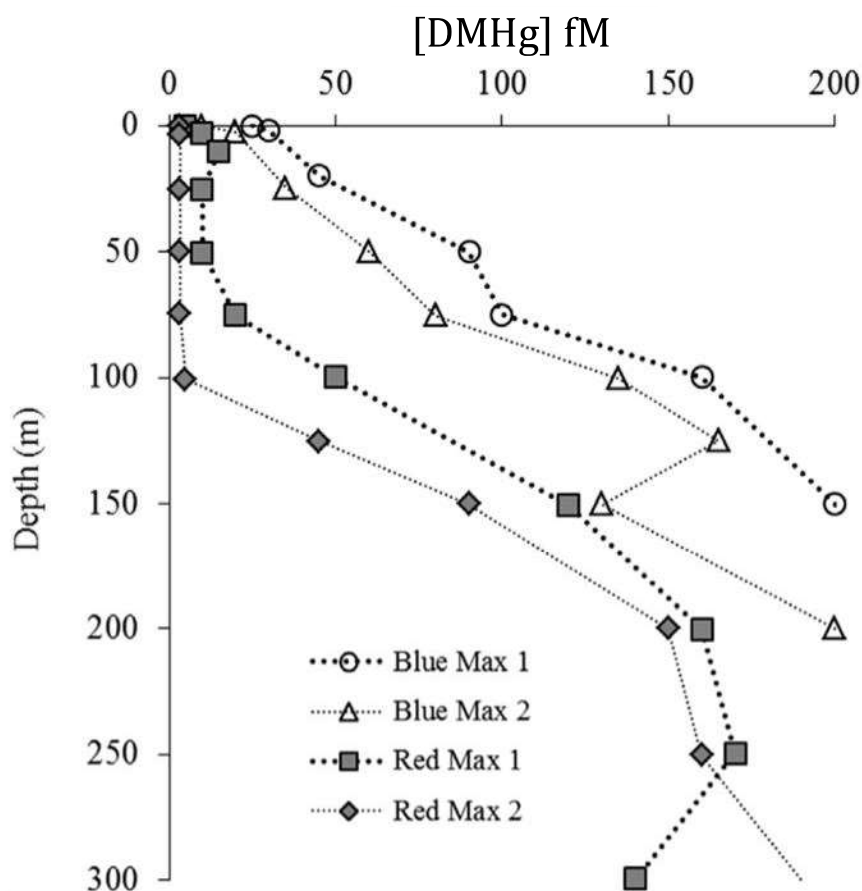
The conditions and mechanisms of surface ocean DMHg conversion to atmospheric MMHg are unknown, however there are probable suspects. Previously observed DMHg loss from sample preservation with HCl solution prompted further study (Fig. 35, Parker and Bloom, 2005; Fitzgerald and Mason, 1997). Black *et al.*, confirmed the finding of DMHg in Monterey Bay surface waters, but also showed minimal DMHg photodemethylation and DMHg to MMHg conversion in acidified samples. While Black *et al.*, used glass in these photodemethylation experiments (which do not transmit UV light), leaving photodemethylation as a potential converter, the exposure to acidic

conditions may provide another chemical pathway (Fig. 36; Black *et al.*, 2009).

Photodemethylation appears to degrade MMHg in aquatic environments (Byington, 2007).

Gradients of DMHg in eddy profiles with surface depletions from 2014-2015 cruises yielded a calculated flux to be $11 \text{ pmol m}^{-2} \text{ d}^{-1}$ (Fig 36.). These are 20x higher than previous values in the literature ($0.2\text{-}0.4 \text{ pmol m}^{-2} \text{ d}^{-1}$, Hammerschmidt & Bowman, 2012), likely due to the “pumping” and accumulative nature of the eddies sampled. Assuming a vertical 100m fog layer, only 0.2% of this flux would be needed to account for MMHg in fog, which can exhibit acidic conditions as low as 2-4 pH (Trumble & Walker, 1991).

Figure 32. DMHg profiles in offshore upwelling and downwelling eddies from 2014-2015 cruises.



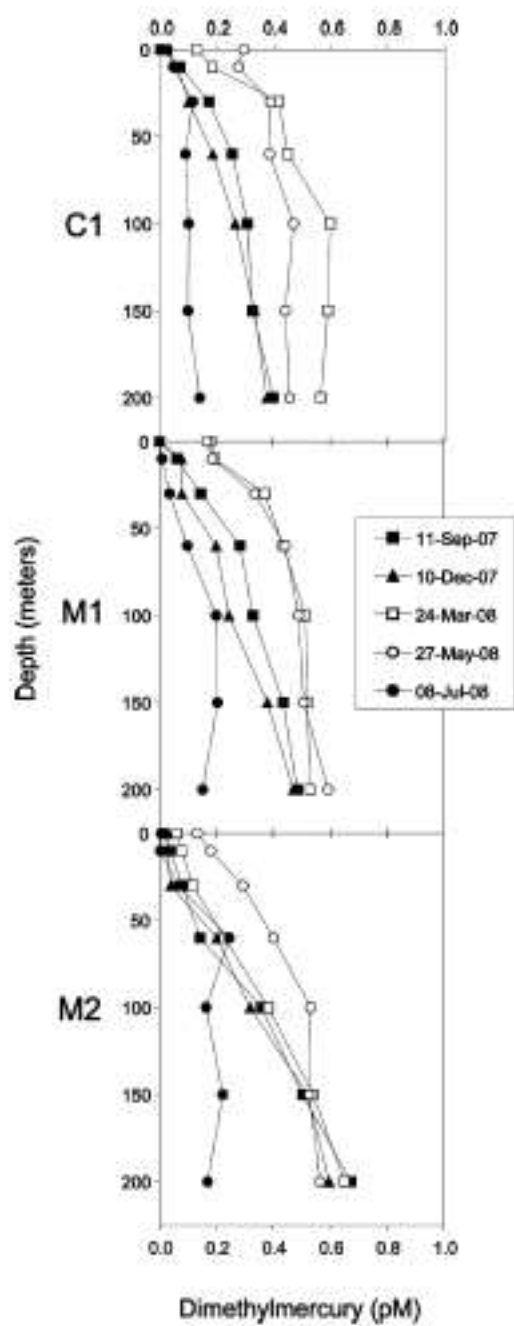
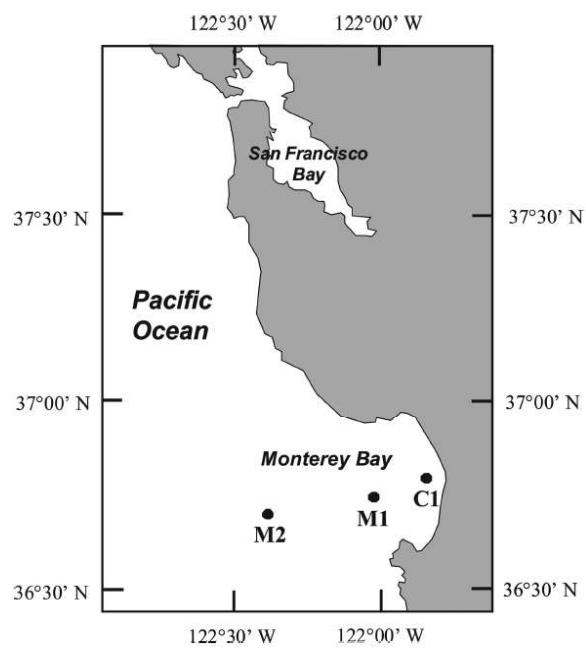


Fig. 33
DMHg profiles in Monterey
Bay. From Conoway *et al.*, 2009



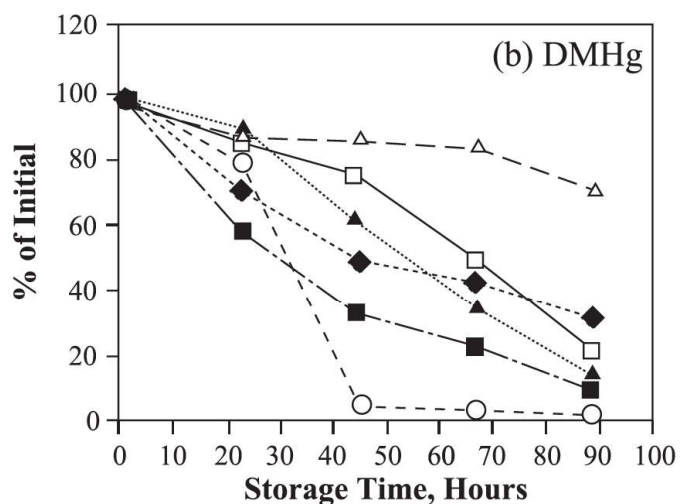
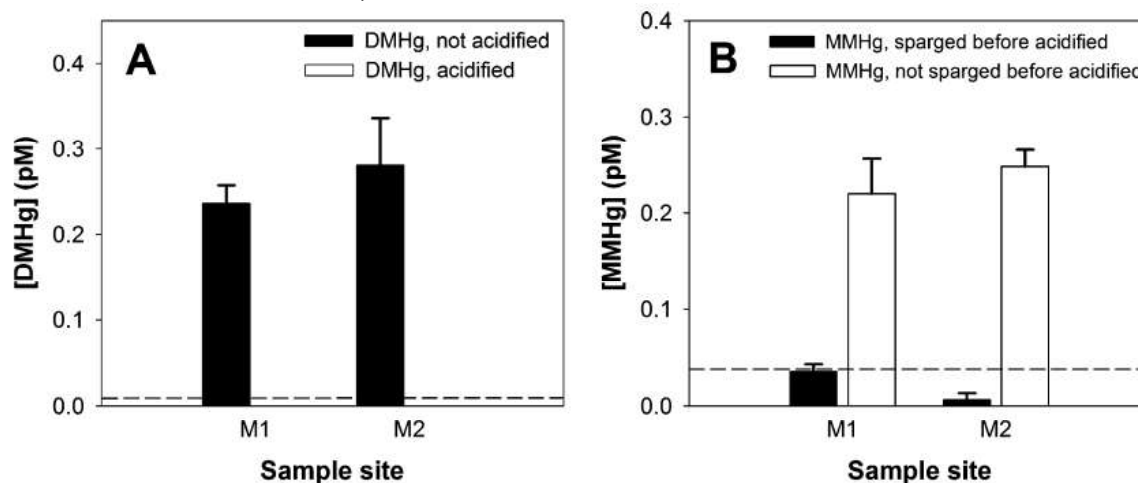


Figure 34. Stability of DMHg in spiked deionized water under different storage conditions. Acidified samples were exposed to room light and temperature, while unpreserved samples were refrigerated in the dark. From Parker & Bloom, 2005.

---◆--- HDPE, no acid —△— Glass, no acid ▲..... Teflon, no acid
 —■— HDPE, 0.4% HCl —□— Glass, 0.4% HCl —○— Teflon, 0.4% HCl

Figure 35. Decrease in DMHg (measured after 4 days) due to acidification and or decomposition of sample (A) was proportional to MMHg measured 3 months later when not initially sparged of DMHg (B). Dashed lines are respective detection limits. From Black *et al.*, 2009



METHODS

To confirm acidification over photodemethylation as a mechanism for DMHg cleavage in the surface seawater and acidic fog conditions, we sought to repeat experimental results from Black *et al.*, 2009. 2-L polycarbonate bottles of natural seawater (pH 7.8–8.2) were incubated in an outdoor tub at natural surface water temperature. Bottle of acidified (pH 5.2) seawater were incubated in a cool, dark area for ~12 hours. Initial and final DMHg and MMHg were also measured using methods described in earlier chapters. Follow-up acidification experiments (pH 1.7 & 3.5) incubated ~300m deep water collected from Monterey Bay in a 25L carboy and incubated again for ~12hrs to replicate a long duration fog event.

RESULTS & DISCUSSION

Our results were comparable to Black *et al.*, with natural unacidified seawater showing no detectable change in DMHg concentrations with time, regardless of the exposure to sunlight. Acidified seawater showed dramatic loss of DMHg under different pH regimes (Fig. 37). Samples from the pH 1.7 follow-up experiment exhibited an increase in MMHg concentrations, and appear to support this paradigm of DMHg demethylation under acidic conditions (Fig. 38). Calculated rate constants from the acidification experiments suggest a higher conversion rate at a lower pH (Fig. 39).

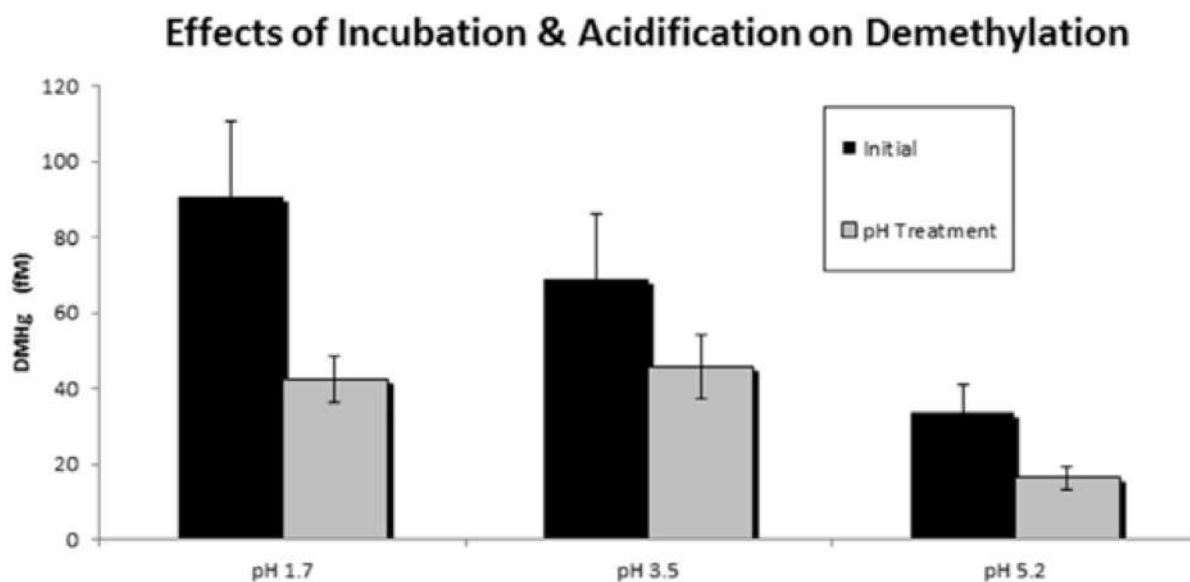


Figure 36. Apparent DMHg loss from acidified seawater incubations. (Coale *et al.*, 2018)

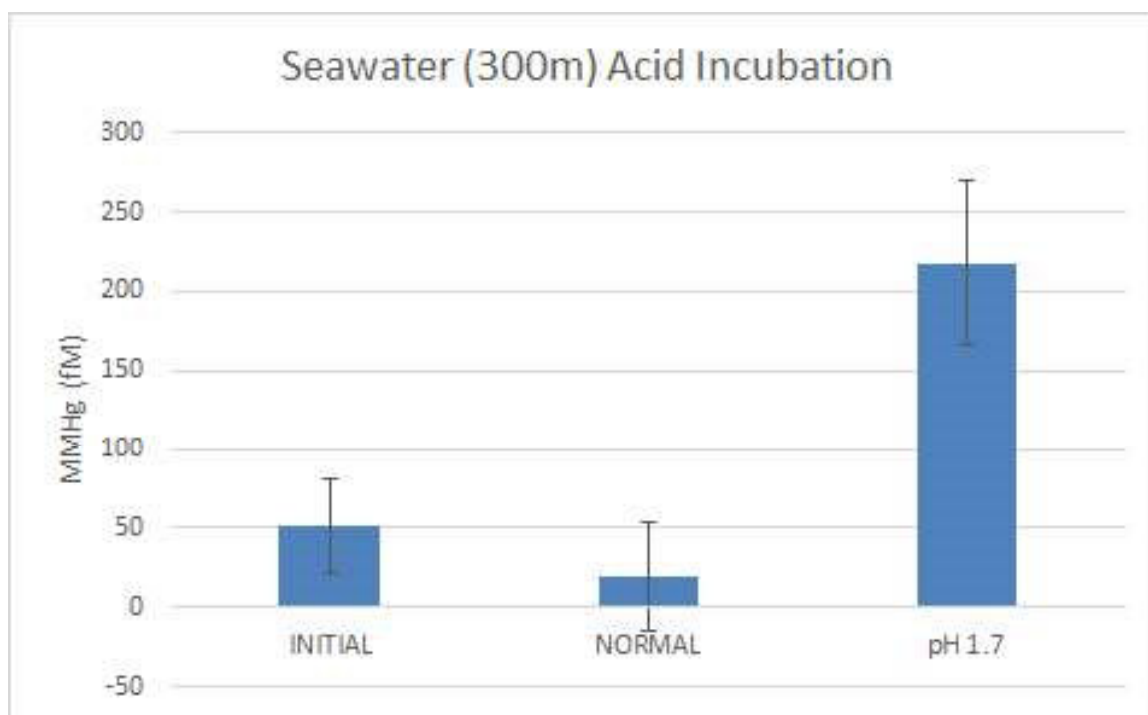


Figure 37. Apparent DMHg conversion to MMHg from acidified seawater (pH 1.7)

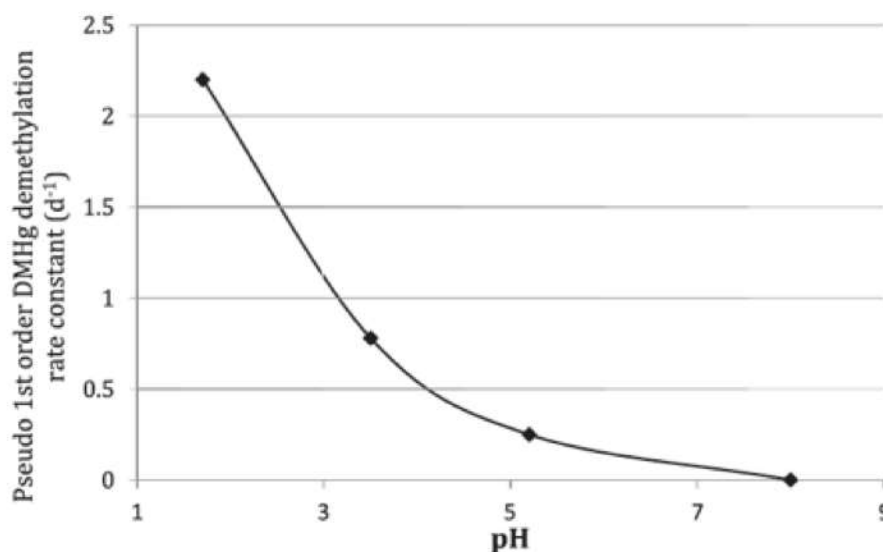


Figure 38. Pseudo first order DMHg demethylation rate constant (d⁻¹) as a function of pH. k_{demeth} (pH=1.7) =2.2 d⁻¹; k_{demeth} (pH 3.5) =0.78 d⁻¹; k_{demeth} (pH 5.2) =0.25d⁻¹; k_{demeth} (pH=8.0) from Black et al. (2009).

Gaseous dimethyl sulfide (DMS) has been known to affect the acidity of the marine boundary layer and thus sea salt aerosols, potentially creating the required acidic (low pH) conditions for DMHg degradation (Fig. 41 Keene *et al.*, 1998; Reid & Sayer, 2002). The DMS precursor dimethylsulfoniopropionate (DMSP) has also been found to be enriched in the SML (Matrai *et al.*, 2008), as it is a product of phytoplankton exudates. DMHg likely evades into the atmosphere and degrades rapidly into MMHg, Hg(II), or Hg⁰ thereafter. This apparent acidolysis-driven demethylation of DMHg into MMHg may explain some, if not most, of the MMHg signal found in fog. Therefore, higher primary productivity could result in higher DMSP-DMS concentrations, and thus DMHg -MMHg conversion over time.

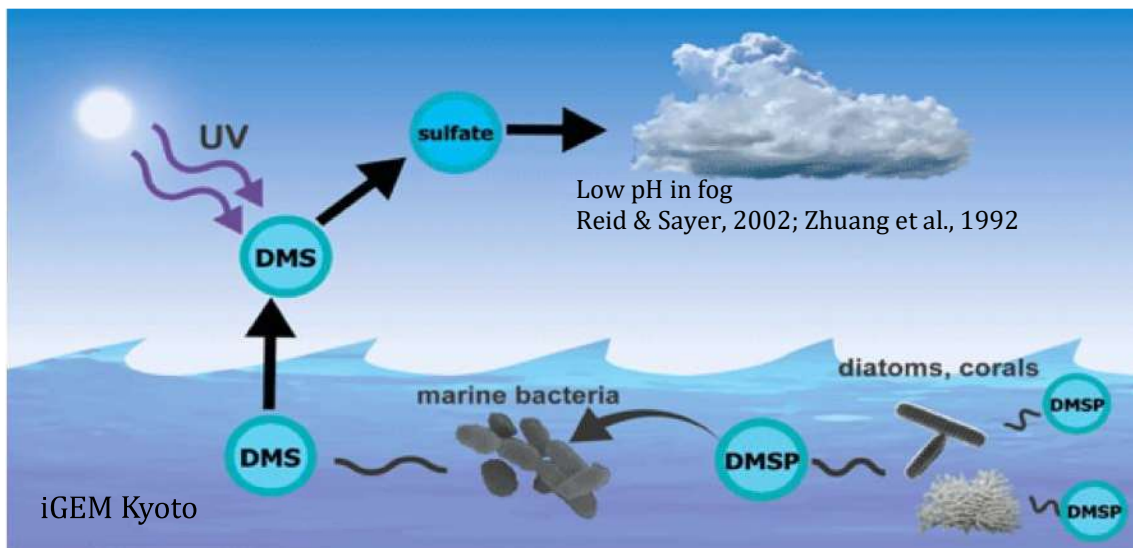


Fig. 39 Dimethyl Sulfide Propionate (DMSP) degradation into Dimethyl Sulfide by marine bacteria, resulting in acidic cloud conditions. Modified from iGEM 2014, Kyoto

CONCLUSION

Evidence of terrestrial biota taking up marine-sourced MMHg through food web bioaccumulation via marine advective fog (Weiss-Penzias, 2012; Rytuba, 2014; Otriz et al. 2014) extends the exposure risk found in seafood to terrestrial organisms. MMHg has been found to greatly affect ecosystem health, disrupting and hampering migratory bird reproduction in the great lakes and as far as the Arctic (Tartu *et al.*, 2013, Scheuhammer *et al.*, 2007) and throughout more locally impacted regions such as the San Francisco Bay Delta complex (Ackerman *et al.*, 2014). Atmospheric deposition of Hg can bioaccumulate noticeably into soil and vegetation within several years (Harris *et al.*, 2007), posing a potential contaminant to nearshore agricultural fields over some period of time. The approximately 25 mile coastal extent of Monterey Bay, where fog can extend 8 miles inland, potentially receives 17g MMHg/ yr. (Fog MMHg flux of $34 \pm 40 \text{ ng m}^{-2} \text{ yr}^{-1}$, Weiss-Penzias et al. 2016).

The coastal zone is extremely complex with various forces synergistically affecting the region. This thesis and related collaborative studies have yielded insight into how these forces and processes appear to influence regional Hg cycling (Fig. 42). 2014-2015 cruises found MMHg and DMHg maxima at 300-800m with concentrations similar to other ocean basins (300-600fm). The uppermost surface layer of the ocean (SML) was found to be enriched up to ~30x, the first measurement of MMHg in that microenvironment and the highest for any heavy metal to date. High levels of pollutants in this heavy organic layer have major implications. Hg, particularly MMHg, adsorbing onto microplastics in the SML also likely elevates levels within the marine food web, not only decreasing health of marine life, but increasing human susceptibility from seafood (Wang *et al.*, 2018). MMHg concentrations and MMHg:THg fractions in fog peak around the near edge coastal zone, essentially in the surf zone. These aerosols may be deposited frequently enough bioaccumulate up the terrestrial food chain.

Results from this thesis suggest that the contribution of MMHg to coastal fog water from aerosolized SML particles is small (~1%) in terms of a MMHg/Cl ratio as a tracer. Gaseous DMHg undergoing acidolysis under low pH atmospheric conditions resulting in particulate MMHg may be the primary pathway of MMHg to fog. However, these contributions may likely fluctuate with the various coastal processes and mechanism intensity, with major factors including shoaling of DMHg and or DMS concentrations (which lower atmospheric pH) during upwelling events as well as primary productivity in the mixed layer (Simó *et. al.*, 1999). Anthropogenic emissions and pollutants in the form of aerosols may also affect fog CCN and pH. To a lesser extent, SML derived MMHg deposition via fog and SSA may also be subject to coastal productivity and water column dynamics that affect the heterogeneity of the SML and SSA (Leeuw *et al.*, 2000). SML and SSA sample sizes were small and require more generous sampling of different conditions to constrain any potential large swings in MMHg terrestrial deposition from fog or sea spray.

While this study finds MMHg concentrations in fog and SML that are thousands fold lower than EPA standards for fish consumption, the areal extent of the coastal zone may, over time, deposit significant levels of particulate MMHg coated aerosols to the coastal landscape. Further determination and quantification of these potential inputs of MMHg, particularly SML and SSA, would refine the uncertainties of global and marine atmospheric Hg cycling (Subir at al., 2011). Understanding the mechanisms and extent of MMHg production and transport is essential to assessing and managing risk of exposure in food webs and human populations.

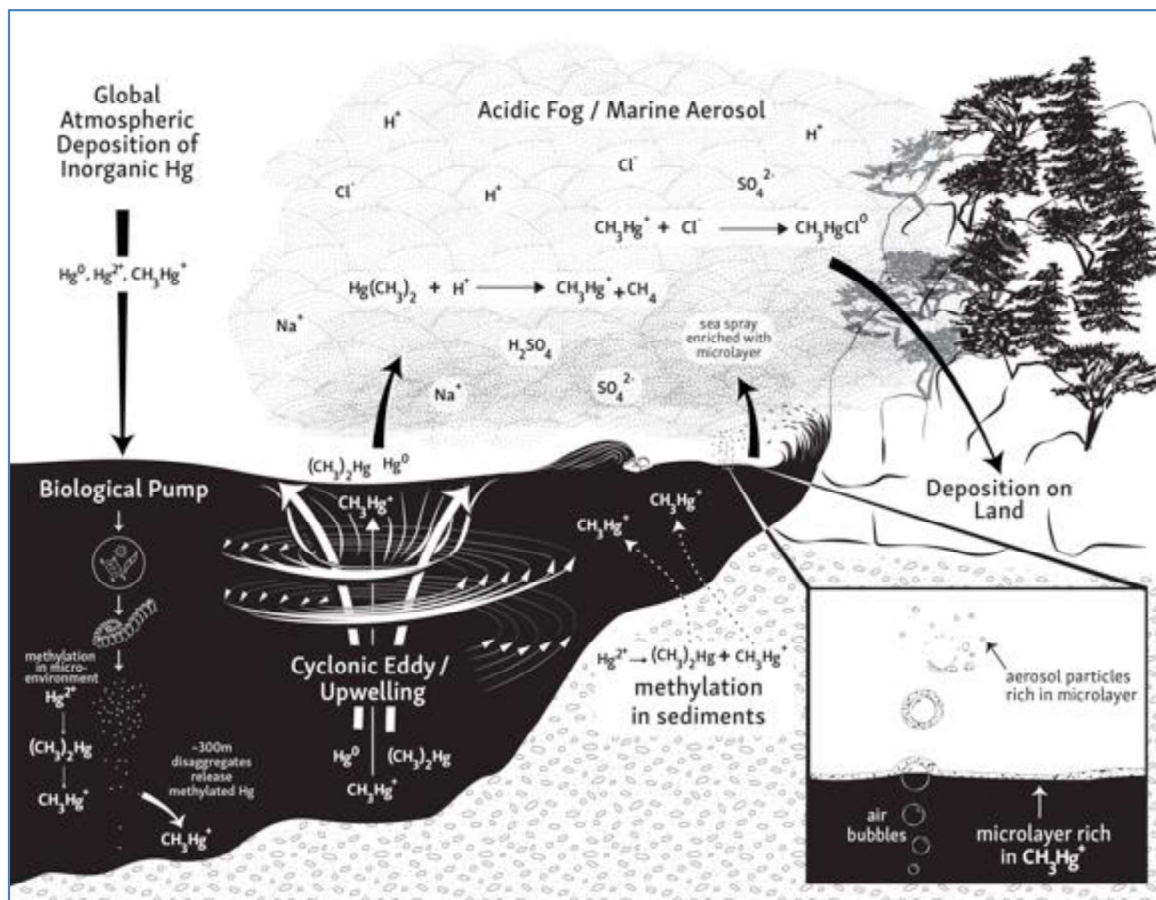


Figure 40. Conceptual model of Hg cycling within the California coastal zone.
 From Coale *et al.*, 2018

References

- Abdel-Shafy, H. I., & Mansour, M. S. (2016). A review on polycyclic aromatic hydrocarbons: source, environmental impact, effect on human health and remediation. *Egyptian Journal of Petroleum*, 25(1), 107-123.
- Ackerman, J. T., Eagles-Smith, C. A., Heinz, G., De La Cruz, S. E., Takekawa, J. Y., Miles, A. K., ... & Maurer, T. C. (2014). *Mercury in birds of San Francisco Bay-Delta, California: trophic pathways, bioaccumulation, and ecotoxicological risk to avian reproduction* (No. 2014-1251). US Geological Survey.
- Aller, J. Y., Kuznetsova, M. R., Jahns, C. J., & Kemp, P. F. (2005). The sea surface microlayer as a source of viral and bacterial enrichment in marine aerosols. *Journal of aerosol science*, 36(5), 801-812.
- Aller, J. Y., Radway, J. C., Kilthau, W. P., Bothe, D. W., Wilson, T. W., Vaillancourt, R. D., ... & Knopf, D. A. (2017). Size-resolved characterization of the polysaccharidic and proteinaceous components of sea spray aerosol. *Atmospheric Environment*, 154, 331-347.
- Alpers, C. N., Hunerlach, M. P., May, J. T., & Hothem, R. L. (2005). Mercury contamination from historical gold mining in California.
- Amos, H. M., Jacob, D. J., Streets, D. G., & Sunderland, E. M. (2013). Legacy impacts of all-time anthropogenic emissions on the global mercury cycle. *Global Biogeochemical Cycles*, 27(2), 410-421.
- Amyot, M., Gill, G. A., & Morel, F. M. (1997). Production and loss of dissolved gaseous mercury in coastal seawater. *Environmental Science & Technology*, 31(12), 3606-3611.
- Aristotle, *Problemata Physica*, Book XXIII "Problems connected with salt water and the sea", No. 38 In Ross, W. D. (Ed. & Trans.1928). *The works of Aristotle translated into English*. (7), 931-936.
- Ariya, P. A., Amyot, M., Dastoor, A., Deeds, D., Feinberg, A., Kos, G., ... & Toyota, K. (2015). Mercury Physicochemical and Biogeochemical Transformation in the Atmosphere and at Atmospheric Interfaces: A Review and Future Directions. *Chemical reviews*.
- Ault, A. P.; Zhao, D.; Ebben, C. J.; Tauber, M. J.; Geiger, F. M.; Prather, K. A.; & Grassian; V. H. (2013). Raman microspectroscopy and vibrational sum frequency generation spectroscopy as probes of the bulk and surface compositions of size-resolved sea spray aerosol particles. *Physical Chemistry Chemical Physics*, 15(17), 6206-6214.
- Azetsu-Scott, K., & Passow, U. (2004). Ascending marine particles: Significance of transparent exopolymer particles (TEP) in the upper ocean. *Limnology and Oceanography*, 49(3), 741-748.

- Baya, P. A., Gosselin, M., Lehnherr, I., St. Louis, V. L., & Hintelmann, H. (2014). Determination of monomethylmercury and dimethylmercury in the Arctic marine boundary layer. *Environmental science & technology*, 49(1), 223-232.
- Black, F. J., Conaway, C. H., & Flegal, A. R. (2009). Stability of dimethyl mercury in seawater and its conversion to monomethyl mercury. *Environmental science & technology*, 43(11), 4056-4062.
- Black, F. J., Paytan, A., Knee, K. L., De Sieyes, N. R., Ganguli, P. M., Gray, E., & Flegal, A. R. (2009). Submarine groundwater discharge of total mercury and monomethylmercury to central California coastal waters. *Environmental science & technology*, 43(15), 5652-5659.
- Blanchard, D. C., & Woodcock, A. H. (1957). Bubble formation and modification in the sea and its meteorological significance. *Tellus*, 9(2), 145-158.
- Blanchard, D. C. & Woodcock, A. H. (1980). THE PRODUCTION, CONCENTRATION, AND VERTICAL DISTRIBUTION OF THE SEA-SALT AEROSOL*. *Annals of the New York Academy of Sciences*, 338(1), 330-347.
- Bowman, K. L., Hammerschmidt, C. R., Lamborg, C. H., & Swarr, G. (2015). Mercury in the North Atlantic Ocean: The US GEOTRACES zonal and meridional sections. *Deep Sea Research Part II: Topical Studies in Oceanography*, 116, 251-261.
- Byington, Amy Adele, "Photo-degradation of methylmercury in the Sacramento-San Joaquin Delta Estuary" (2007). Master's Theses. Paper 3368.
- Choe, K. Y., Gill, G. A., Lehman, R. D., Han, S., Heim, W. A., & Coale, K. H. (2004). Sediment-water exchange of total mercury and monomethyl mercury in the San Francisco Bay-Delta. *Limnology and Oceanography*, 49(5), 1512-1527.
- Chow, J. C., & Watson, J. G. (2017). Enhanced Ion Chromatographic Speciation of Water-Soluble PM_{2.5} to Improve Aerosol Source Apportionment. *Aerosol Science and Engineering*, 1(1), 7-24.
- Carlson, D. J. (1982). Phytoplankton in marine surface microlayers. *Canadian Journal of Microbiology*, 28(11), 1226-1234.
- Coale, K. H., Heim, W. A., Negrey, J., Weiss-Penzias, P., Fernandez, D., Olson, A., ... & Newman, A. (2018). The distribution and speciation of mercury in the California Current: Implications for mercury transport via fog to land. *Deep Sea Research Part II: Topical Studies in Oceanography*.

- Coale, K. H., Heim, W. A., Olson, A., Chiswell, H., Byington, A., Newman, A., ... & Parker, C. (2015, December). Dimethyl Mercury in Seawater: a Potential Source of Monomethyl Mercury in Fog. In *AGU Fall Meeting Abstracts*.
- Cole, M., Lindeque, P., Fileman, E., Halsband, C., Goodhead, R., Moger, J., & Galloway, T. S. (2013). Microplastic ingestion by zooplankton. *Environmental science & technology*, 47(12), 6646-6655.
- Compeau, G. C. & Bartha, R. (1985). Sulfate-reducing bacteria: principal methylators of mercury in anoxic estuarine sediment. *Applied and environmental microbiology*, 50(2), 498-502.
- Cullen, J. J., MacIntyre, H. L., & Carlson, D. J. (1989). Distributions and photosynthesis of phototrophs in sea-surface films. *Marine Ecology Progress Series*, 271-278.
- Cunliffe, M., & Murrell, J. C. (2009). The sea-surface microlayer is a gelatinous biofilm. *The ISME Journal*, 3(9), 1001.
- Cunliffe, M., Engel, A., Frka, S., Gašparović, B., Guitart, C., Murrell, J. C., ... & Wurl, O. (2013). Sea surface microlayers: A unified physicochemical and biological perspective of the air–ocean interface. *Progress in Oceanography*, 109, 104-116.
- Dawson, T. E. (1998). Fog in the California redwood forest: ecosystem inputs and use by plants. *Oecologia*, 117(4), 476-485.
- Demoz, B. B., Collett, J. L., & Daube, B. C. (1996). On the Caltech active strand cloudwater collectors. *Atmospheric Research*, 41(1), 47-62.
- Driscoll, C. T.; Mason, R. P.; Chan, H. M.; Jacob, D. J.; & Pirrone, N. (2013). Mercury as a global pollutant: sources, pathways, and effects. *Environmental science & technology*, 47(10), 4967-4983.
- Drevnick, P. E., Lamborg, C. H., & Horgan, M. J. (2015). Increase in mercury in Pacific yellowfin tuna. *Environmental Toxicology and Chemistry*, 34(4), 931-934.
- Ebling, A. M., & Landing, W. M. (2015). Sampling and analysis of the sea surface microlayer for dissolved and particulate trace elements. *Marine Chemistry*.
- Ebling, A. M., & Landing, W. M. (2017). Trace elements in the sea surface microlayer: rapid responses to changes in aerosol deposition.
- Engel, A., Bange, H. W., Cunliffe, M., Burrows, S. M., Friedrichs, G., Galgani, L., ... & Quinn, P. K. (2017). The ocean's vital skin: Toward an integrated understanding of the sea surface microlayer. *Frontiers in Marine Science*, 4, 165.

FAO (Food and Agriculture Organization of the United Nations). (2014). The State of World Fisheries and Aquaculture.

Fisher, N. S., & Reinfelder, J. R. (1995). The trophic transfer of metals in marine systems. *Metal speciation and bioavailability in aquatic systems*, 3, 407-411.

Fitzgerald, W. F., Lamborg, C. H., & Hammerschmidt, C. R. (2007). Marine biogeochemical cycling of mercury. *Chemical Reviews*, 107(2), 641-662.

Franklin, B., & Brownrigg, W. (1774). XLIV. Of the stilling of waves by means of oil. Extracted from sundry letters between Benjamin Franklin, LL. DFRS William Brownrigg, MDRS and the Reverend Mr. Farish. *Philosophical Transactions of the Royal Society of London*, (64), 445-460.

Fuentes, E., Coe, H., Green, D., Leeuw, G. D., & McFiggans, G. (2010). On the impacts of phytoplankton-derived organic matter on the properties of the primary marine aerosol—Part 1: Source fluxes. *Atmospheric Chemistry and Physics*, 10(19), 9295-9317.

Galgani, L. & Engel, A. (2013). "Accumulation of Gel Particles in the Sea-Surface Microlayer during an Experimental Study with the Diatom *Thalassiosira weissflogii*," *International Journal of Geosciences*, 4(1), pp. 129-145.

Galgani, L., Stolle, C., Endres, S., Schulz, K. G., & Engel, A. (2014). Effects of ocean acidification on the biogenic composition of the sea-surface microlayer: Results from a mesocosm study. *Journal of Geophysical Research: Oceans*, 119(11), 7911-7924.

Ganguli, P. M., Conaway, C. H., Swarzenski, P. W., Izbicki, J. A., & Flegal, A. R. (2012). Mercury speciation and transport via submarine groundwater discharge at a Southern California coastal lagoon system. *Environmental science & technology*, 46(3), 1480-1488.

Gantt, B., Meskhidze, N., Facchini, M. C., Rinaldi, M., Ceburnis, D., & O'Dowd, C. D. (2011). Wind speed dependent size-resolved parameterization for the organic mass fraction of sea spray aerosol. *Atmospheric Chemistry and Physics*, 11(16), 8777-8790.

Garbe, C. S., Rutgersson, A., Boutin, J., De Leeuw, G., Delille, B., Fairall, C. W., ... & Nightingale, P. D. (2014). Transfer across the air-sea interface. In *Ocean-Atmosphere interactions of gases and particles* (pp. 55-112). Springer, Berlin, Heidelberg.

García, O., Veiga, M. M., Cordy, P., Suescún, O. E., Molina, J. M., & Roeser, M. (2015). Artisanal gold mining in Antioquia, Colombia: a successful case of mercury reduction. *Journal of Cleaner Production*, 90, 244-252.

Gilmour, C. C., Bullock, A. L., McBurney, A., Podar, M., & Elias, D. A. (2018). Robust Mercury Methylation across Diverse Methanogenic Archaea. *MBio*, 9(2), e02403-17.

Gilmour, C. C., Elias, D. A., Kucken, A. M., Brown, S. D., Palumbo, A. V., Schadt, C. W., & Wall, J. D. (2011). Sulfate-reducing bacterium *Desulfovibrio desulfuricans* ND132 as a model for understanding bacterial mercury methylation. *Applied and environmental microbiology*, 77(12), 3938-3951.

Hammerschmidt, C. R., & Bowman, K. L. (2012). Vertical methylmercury distribution in the subtropical North Pacific Ocean. *Marine Chemistry*, 132, 77-82.

Hardy, J. T., Apts, C. W., Crecelius, E. A., & Bloom, N. S. (1985). Sea-surface microlayer metals enrichments in an urban and rural bay. *Estuarine, Coastal and Shelf Science*, 20(3), 299-312.

Hardy, J. T., & Apts, C. W. (1989). Photosynthetic carbon reduction: high rates in the sea-surface microlayer. *Marine Biology*, 101(3), 411-417.

Hardy, J. T., Crecelius, E. A., Antrim, L. D., Kiesser, S. L., Broadhurst, V. L., Boehm, P. D., ... & Coogan, T. H. (1990). Aquatic surface microlayer contamination in Chesapeake Bay. *Marine Chemistry*, 28(4), 333-351.

Hardy, J. T., & Cleary, J. (1992). Surface microlayer contamination and toxicity in the German Bight. *Marine Ecology Progress Series*, 203-210.

Harris, R. C., Rudd, J. W., Amyot, M., Babiarz, C. L., Beaty, K. G., Blanchfield, P. J., ... & Heyes, A. (2007). Whole-ecosystem study shows rapid fish-mercury response to changes in mercury deposition. *Proceedings of the National Academy of Sciences*, 104(42), 16586-16591.

Harvey, G. W. & Burzell, L. A. (1972). A SIMPLE MICROLAYER METHOD FOR SMALL SAMPLES¹. *Limnology and Oceanography*, 17(1), 156-157.

Heim, W. A., Weiss-Penzias, P. S., Fernandez, D., Byington, A., Bonnema, A., Beebe, C., ... & Coale, K. H. (2014, December). Is the Coastal Ocean a Source of Mercury to Marine Advective Fog. In *AGU Fall Meeting Abstracts*.

Heimbürger, L. E., Cossa, D., Marty, J. C., Migon, C., Averty, B., Dufour, A., & Ras, J. (2010). Methyl mercury distributions in relation to the presence of nano-and picophytoplankton in an oceanic water column (Ligurian Sea, North-western Mediterranean). *Geochimica et Cosmochimica Acta*, 74(19), 5549-5559.

Horowitz, H. M., Jacob, D. J., Amos, H. M., Streets, D. G., & Sunderland, E. M. (2014). Historical mercury releases from commercial products: Global environmental implications. *Environmental science & technology*, 48(17), 10242-10250.

Horvat, M., Liang, L., & Bloom, N. S. (1993). Comparison of distillation with other current isolation methods for the determination of methyl mercury compounds in low level environmental samples: Part II. Water. *Analytica Chimica Acta*, 282(1), 153-168.

Ingraham, N. L.; & Matthews, R. A. (1995). The importance of fog-drip water to vegetation: Point Reyes Peninsula, California. *Journal of Hydrology*, 164(1), 269-285.

Johengen, T., Smith, G. J., Purcell, H., Loranger, S., Gilbert, S., Maurer, T., ... & Tamburri, M. (2012). *Performance Verification Statement for the Chelsea UviLux Hydrocarbon and CDOM Fluorometers*.

Keene, W. C., Sander, R., Pszenny, A. A., Vogt, R., Crutzen, P. J., & Galloway, J. N. (1998). Aerosol pH in the marine boundary layer: A review and model evaluation. *Journal of Aerosol Science*, 29(3), 339-356.

Kim, M. K., & Zoh, K. D. (2012). Fate and transport of mercury in environmental media and human exposure. *Journal of Preventive Medicine and Public Health*, 45(6), 335.

Kinsey, J. D., Corradino, G., Ziervogel, K., Schnetzer, A., & Osburn, C. L. (2018). Formation of chromophoric dissolved organic matter by bacterial degradation of phytoplankton-derived aggregates. *Frontiers in Marine Science*, 4, 430.

Lamborg, C. H., Fitzgerald, W. F., Damman, A. W. H., Benoit, J. M., Balcom, P. H., & Engstrom, D. R. (2002). Modern and historic atmospheric mercury fluxes in both hemispheres: global and regional mercury cycling implications. *Global Biogeochemical Cycles*, 16(4).

Lamborg, C. H., Hammerschmidt, C. R., Gill, G. A., Mason, R. P., & Gichuki, S. (2012). An intercomparison of procedures for the determination of total mercury in seawater and recommendations regarding mercury speciation during GEOTRACES cruises. *Limnology and Oceanography: Methods*, 10(2), 90-100.

Lamborg, C. H., Kent, D. B., Swarr, G. J., Munson, K. M., Kading, T., O'Connor, A. E., ... & Wiatrowski, H. A. (2013). Mercury speciation and mobilization in a wastewater-contaminated groundwater plume. *Environmental science & technology*, 47(23), 13239-13249.

Lamborg, C. H., Bowman, K., Hammerschmidt, C. R., Gilmour, C., Munson, K. M., Selin, N., & Tseng, C. M. (2014). Mercury in the anthropocene ocean.

Lamborg, C. H., Hammerschmidt, C. R., Bowman, K. L., Swarr, G. J., Munson, K. M., Ohnemus, D. C., ... & Saito, M. A. (2014). A global ocean inventory of anthropogenic mercury based on water column measurements. *Nature*, 512(7512), 65-68.

Lamborg, C. H., Hammerschmidt, C. R., & Bowman, K. L. (2016). An examination of the role of particles in oceanic mercury cycling. *Phil. Trans. R. Soc. A*, 374(2081), 20150297.

- Laskin, A., Moffet, R. C., Gilles, M. K., Fast, J. D., Zaveri, R. A., Wang, B., ... & Shutthanandan, J. (2012). Tropospheric chemistry of internally mixed sea salt and organic particles: Surprising reactivity of NaCl with weak organic acids. *Journal of Geophysical Research: Atmospheres*, 117(D15).
- Lasorsa, B., & Allen-Gil, S. (1995). The methylmercury to total mercury ratio in selected marine, freshwater, and terrestrial organisms. *Water, Air, and Soil Pollution*, 80(1-4), 905-913.
- Lee, C. S., & Fisher, N. S. (2017). Bioaccumulation of methylmercury in a marine diatom and the influence of dissolved organic matter. *Marine Chemistry*, 197, 70-79.
- Lee, J. I., Yang, J. H., Kim, P. R., & Han, Y. J. (2018). Effects of organic carbon and UV wavelength on the formation of dissolved gaseous mercury in water under a controlled environment. *Environmental Engineering Research*, 24(1), 54-62.
- Leeuw, G., Neele, F. P., Hill, M., Smith, M. H., & Vignati, E. (2000). Production of sea spray aerosol in the surf zone. *Journal of Geophysical Research: Atmospheres*, 105(D24), 29397-29409.
- Mason, R. P., & Fitzgerald, W. F. (1993). The distribution and biogeochemical cycling of mercury in the equatorial Pacific Ocean. *Deep Sea Research Part I: Oceanographic Research Papers*, 40(9), 1897-1924.
- Mason, R. P., Fitzgerald, W. F., & Morel, F. M. (1994). The biogeochemical cycling of elemental mercury: anthropogenic influences. *Geochimica et Cosmochimica Acta*, 58(15), 3191-3198.
- Mason, R. P.; Reinfelder, J. R.; & Morel, F. M. (1996). Uptake, toxicity, and trophic transfer of mercury in a coastal diatom. *Environmental Science & Technology*, 30(6), 1835-1845.
- Mason, R. P., Choi, A. L., Fitzgerald, W. F., Hammerschmidt, C. R., Lamborg, C. H., Soerensen, A. L., & Sunderland, E. M. (2012). Mercury biogeochemical cycling in the ocean and policy implications. *Environmental research*, 119, 101-117.
- Mason, R. P., Hammerschmidt, C. R., Lamborg, C. H., Bowman, K. L., Swarr, G. J., & Shelley, R. U. (2017). The air-sea exchange of mercury in the low latitude Pacific and Atlantic Oceans. *Deep Sea Research Part I: Oceanographic Research Papers*, 122, 17-28.
- Matrai, P. A., Tranvik, L., Leck, C., & Knulst, J. C. (2008). Are high Arctic surface microlayers a potential source of aerosol organic precursors? *Marine Chemistry*, 108(1-2), 109-122.

- Migon, C., & Nicolas, E. (1998). The trace metal recycling component in the north-western Mediterranean. *Marine Pollution Bulletin*, 36(4), 273-277.
- Miranda, M. L., Mustaffa, N. I. H., Robinson, T. B., Stolle, C., Ribas-Ribas, M., Wurl, O., & Zielinski, O. (2018). Influence of solar radiation on biogeochemical parameters and fluorescent dissolved organic matter (FDOM) in the sea surface microlayer of the southern coastal North Sea. *Elem Sci Anth*, 6(1).
- Monperrus, M., Tessier, E., Amouroux, D., Leynaert, A., Huonnic, P., & Donard, O. F. X. (2007). Mercury methylation, demethylation and reduction rates in coastal and marine surface waters of the Mediterranean Sea. *Marine Chemistry*, 107(1), 49-63.
- Moye, H. A., Miles, C. J., Philips, E. J., Sargent, B., & Merritt, K. K. (2002). Kinetics and uptake mechanisms for monomethylmercury between freshwater algae and water. *Environmental science & technology*, 36(16), 3550-3555.
- Munson, K. M., Babi, D., & Lamborg, C. H. (2014). Determination of monomethylmercury from seawater with ascorbic acid-assisted direct ethylation. *Limnology and Oceanography: Methods*, 12(1), 1-9.
- Mustaffa, N. I. H., Badewien, T. H., Ribas-Ribas, M., & Wurl, O. (2018). High-resolution observations on enrichment processes in the sea-surface microlayer. *Scientific reports*, 8(1), 13122.
- Obrist, D., Kirk, J. L., Zhang, L., Sunderland, E. M., Jiskra, M., & Selin, N. E. (2018). A review of global environmental mercury processes in response to human and natural perturbations: Changes of emissions, climate, and land use. *Ambio*, 1-25.
- Oczkowski, A., Kreakie, B., McKinney, R. A., & Prezioso, J. (2016). Patterns in stable isotope values of nitrogen and carbon in particulate matter from the Northwest Atlantic continental shelf, from the Gulf of Maine to Cape Hatteras. *Frontiers in Marine Science*, 3, 252.
- Ortiz Jr, C.; Weiss-Penzias, P. S.; Fork, S.; & Flegal, A. R. (2014). Total and Monomethyl Mercury in Terrestrial Arthropods from the Central California Coast. *Bulletin of environmental contamination and toxicology*, 1-6.
- Parks, J. M., Johs, A., Podar, M., Bridou, R., Hurt, R. A., Smith, S. D., ... & Liang, L. (2013). The genetic basis for bacterial mercury methylation. *Science*, 339(6125), 1332-1335.
- Prather, K. A.; Bertram, T. H.; Grassian, V. H.; Deane, G. B.; Stokes, M. D.; DeMott, P. J., ... & Zhao, D. (2013). Bringing the ocean into the laboratory to probe the chemical complexity of sea spray aerosol. *Proceedings of the National Academy of Sciences*, 110(19), 7550-7555.

Prospero, J. M. (2002). The chemical and physical properties of marine aerosols: An introduction. In *Chemistry of Marine Water and Sediments* (pp. 35-82). Springer Berlin Heidelberg.

Pickhardt, P. C., & Fisher, N. S. (2007). Accumulation of inorganic and methylmercury by freshwater phytoplankton in two contrasting water bodies. *Environmental science & technology*, 41(1), 125-131.

Pirrone, N., Cinnirella, S., Feng, X., Finkelman, R. B., Friedli, H. R., Leaner, J., ... & Telmer, K. (2010). Global mercury emissions to the atmosphere from anthropogenic and natural sources. *Atmospheric Chemistry and Physics*, 10(13), 5951-5964.

Reid, J. P., & Sayer, R. M. (2002). Chemistry in the clouds: the role of aerosols in atmospheric chemistry. *Science progress*, 85(3), 263-296.

Renzoni, A., Zino, F., & Franchi, E. (1998). Mercury levels along the food chain and risk for exposed populations. *Environmental Research*, 77(2), 68-72.

Rytuba, J. J. (2014, December). Naturally Elevated Monomethylmercury and Mercury Concentrations of Redwood Trees of Coastal California. In *AGU Fall Meeting Abstracts* (Vol. 1, p. 0303).

Scheuhammer, A. M., Meyer, M. W., Sandheinrich, M. B., & Murray, M. W. (2007). Effects of environmental methylmercury on the health of wild birds, mammals, and fish. *AMBIO: A Journal of the Human Environment*, 36(1), 12-19.

Scheuhammer, A. M. (1991). Effects of acidification on the availability of toxic metals and calcium to wild birds and mammals. *Environmental Pollution*, 71(2), 329-375.

Seaber, P. R., Kapinos, F. P., & Knapp, G. L. (1987). Hydrologic unit maps. USGS Water Supply Paper 2294. *US Geological Survey, Corvallis, OR*.

Seigneur, C., Vijayaraghavan, K., Lohman, K., Karamchandani, P., & Scott, C. (2004). Global source attribution for mercury deposition in the United States. *Environmental Science & Technology*, 38(2), 555-569.

Shiuan, C., & Nicholas, S. (2017). Bioaccumulation of methylmercury in a marine copepod. *Environmental toxicology and chemistry*.

Simó, R., & Pedrós-Alió, C. (1999). Role of vertical mixing in controlling the oceanic production of dimethyl sulphide. *Nature*, 402(6760), 396.

Song, Y. K., Hong, S. H., Jang, M., Han, G. M., & Shim, W. J. (2015). Occurrence and distribution of microplastics in the sea surface microlayer in Jinhae Bay, South Korea. *Archives of environmental contamination and toxicology*, 69(3), 279-287.

Steding, D. J., & Flegal, A. R. (2002). Mercury concentrations in coastal California precipitation: Evidence of local and trans-Pacific fluxes of mercury to North America. *Journal of Geophysical Research: Atmospheres* (1984–2012), 107(D24), ACH-11.

Stortini, A. M., Cincinelli, A., Degli Innocenti, N., Tovar-Sánchez, A., & Knulst, J. (2012). Surface microlayer.

St. Pierre, K. A., St. Louis, V. L., Kirk, J. L., Lehnherr, I., Wang, S., & La Farge, C. (2015). Importance of open marine waters to the enrichment of total mercury and monomethylmercury in lichens in the Canadian High Arctic. *Environmental science & technology*, 49(10), 5930-5938.

Subir, M., Ariya, P. A., & Dastoor, A. P. (2011). A review of uncertainties in atmospheric modeling of mercury chemistry I. Uncertainties in existing kinetic parameters—Fundamental limitations and the importance of heterogeneous chemistry. *Atmospheric Environment*, 45(32), 5664-5676.

Subir, M., Ariya, P. A., & Dastoor, A. P. (2012). A review of the sources of uncertainties in atmospheric mercury modeling II. Mercury surface and heterogeneous chemistry—A missing link. *Atmospheric Environment*, 46, 1-10.

Sun, L., Yin, X., Liu, X., Zhu, R., Xie, Z., & Wang, Y. (2006). A 2000-year record of mercury and ancient civilizations in seal hairs from King George Island, West Antarctica. *Science of the Total Environment*, 368(1), 236-247.

Sunderland, E. M., Krabbenhoft, D. P., Moreau, J. W., Strode, S. A., & Landing, W. M. (2009). Mercury sources, distribution, and bioavailability in the North Pacific Ocean: Insights from data and models. *Global Biogeochemical Cycles*, 23(2).

Tartu, S., Goutte, A., Bustamante, P., Angelier, F., Moe, B., Clément-Chastel, C., ... & Chastel, O. (2013). To breed or not to breed: endocrine response to mercury contamination by an Arctic seabird. *Biology letters*, 9(4), 20130317.

Thornton, D. C. (2014). Dissolved organic matter (DOM) release by phytoplankton in the contemporary and future ocean. *European Journal of Phycology*, 49(1), 20-46.

Tilstone, G. H., Airs, R. L., Vicente, V. M., Widdicombe, C., & Llewellyn, C. (2010). High concentrations of mycosporine-like amino acids and colored dissolved organic matter in the sea surface microlayer off the Iberian Peninsula. *Limnology and Oceanography*, 55(5), 1835-1850.

Topping, G.; Davies, I. M. (1981) Methylmercury production in the water column. *Nature* 1981, 290, 243.

- Tovar-Sánchez, A., Arrieta, J. M., Duarte, C. M., & Sañudo-Wilhelmy, S. A. (2014). Spatial gradients in trace metal concentrations in the surface microlayer of the Mediterranean Sea. *Frontiers in Marine Science*, 1, 79.
- Trumble, J. T., & Walker, G. P. (1991). Acute effects of acidic fog on photosynthetic activity and morphology of *Phaseolus lunatus*. *HortScience*, 26(12), 1531-1534.
- US Environmental Protection Agency (EPA). Methylmercury (MMHg) [CASRN 22967-92-6]. Washington (DC): Integrated Risk Information System, EPA; 2001.
- Wang, X., Deane, G. B., Moore, K. A., Ryder, O. S., Stokes, M. D., Beall, C. M., ... & Prather, K. A. (2017). The role of jet and film drops in controlling the mixing state of submicron sea spray aerosol particles. *Proceedings of the National Academy of Sciences*, 114(27), 6978-6983.
- Wang, F., Wang, F., & Zeng, E. Y. (2018). Sorption of Toxic Chemicals on Microplastics. In *Microplastic Contamination in Aquatic Environments* (pp. 225-247).
- Weiss-Penzias, P. S., Ortiz, C., Acosta, R. P., Heim, W., Ryan, J. P., Fernandez, D., ... & Flegal, A. R. (2012). Total and monomethyl mercury in fog water from the central California coast. *Geophysical Research Letters*, 39(3).
- Weiss-Penzias, P., Coale, K., Heim, W., Fernandez, D., Oliphant, A., Dodge, C., ... & Olson, A. (2016). Total-and monomethyl-mercury and major ions in coastal California fog water: Results from two years of sampling on land and at sea. *Elem Sci Anth*, 4.
- Weiss-Penzias, P., Sorooshian, A., Coale, K., Heim, W., Crosbie, E., Dadashazar, H., ... & Jonsson, H. (2018). Aircraft Measurements of Total Mercury and Monomethyl Mercury in Summertime Marine Stratus Cloudwater from Coastal California, USA. *Environmental science & technology*, 52(5), 2527-2537.
- Witt, S. F. (1991). OSHA safety hazard information bulletin on dimethylmercury. Washington, DC: US Department of Labor. Occupational Safety and Health Administration, 1.
- Wurl, O., & Obbard, J. P. (2004). A review of pollutants in the sea-surface microlayer (SML): a unique habitat for marine organisms. *Marine Pollution Bulletin*, 48(11), 1016-1030.
- Wurl, O., Wurl, E., Miller, L., Johnson, K., & Vagle, S. (2011). Formation and global distribution of sea-surface microlayers. *Biogeosciences*, 8(1), 121.
- Wurl, O., Ekau, W., Landing, W. M., & Zappa, C. J. (2017). Sea surface microlayer in a changing ocean—A perspective. *Elem Sci Anth*, 5.

Zäncker, B., Bracher, A., Röttgers, R., & Engel, A. (2017). Variations of the organic matter composition in the sea surface microlayer: a comparison between open ocean, coastal, and upwelling sites off the Peruvian coast. *Frontiers in microbiology*, 8, 2369.

Zhou, J., Mopper, K., & Passow, U. (1998). The role of surface-active carbohydrates in the formation of transparent exopolymer particles by bubble adsorption of seawater. *Limnology and Oceanography*, 43(8), 1860-1871.

Zhuang, G., Yi, Z., Duce, R. A., & Brown, P. R. (1992). Link between iron and sulphur cycles suggested by detection of Fe (n) in remote marine aerosols. *Nature*, 355(6360), 537

APPENDIX A

Table 3. 2014-2015 station locations and sampling dates

Station Name	Date	Lat (°N)	Lon (°W)
Brazil Ranch	05/06/2014	36.27	121.96
Canyon Axis	06/06/2014	36.62	122.38
Long Marine	06/06/2014	36.95	122.20
San Mateo Shelf	07/06/2014	37.12	122.84
Montara	07/06/2014	37.53	122.57
Bodega	08/06/2014	38.31	123.13
Cordell Bank	08/06/2014	37.88	123.25
Pepperwood	08/06/2014	38.57	123.43
Shelter Cove	09/06/2014	40.01	124.15
Cape Mendocino	10/06/2014	40.44	124.53
Eureka Shelf	11/06/2014	40.83	124.36
Trinidad Upwelling	11/06/2014	41.50	124.25
Blue Max 1	12/08/2014	41.89	124.92
Red Max 1	13/08/2014	42.20	126.86
Cape Mendocino	14/08/2014	40.44	124.53
Eureka Shelf	14/08/2014	40.83	124.36
Red Max 2	14/08/2014	39.85	125.63
Blue Max 2	15/08/2014	39.14	124.57
Pepperwood	15/08/2014	38.57	123.43
Red Max 2	15/08/2014	39.85	125.63
Bodega-2	16/08/2014	38.31	123.13
Cordell Bank-2	16/08/2014	37.88	123.25
Montara	16/08/2014	37.53	122.57
Canyon Axis	17/08/2014	36.62	122.38
Long Marine Lab	17/08/2014	36.93	122.04
San Mateo Shelf	17/08/2014	37.12	122.84
Brazil Ranch-2	18/08/2014	36.52	122.01
Pt Sur	18/08/2014	36.24	121.89
Canyon Axis	24/06/2015	36.62	122.40

Long Marine Lab	24/06/2015	36.90	122.09
Bodega	25/06/2015	38.30	123.13
Montara	25/06/2015	37.68	122.59
Caspar Point	26/06/2015	39.37	123.94
Eureka	26/06/2015	40.84	124.36
Crescent	27/06/2015	41.76	125.47
Mendocino	27/06/2015	40.51	125.27
Cabrillo	28/06/2015	39.39	125.10
Pt Reyes	28/06/2015	38.00	125.00
Monterey	29/06/2015	36.67	124.16
Soberanes	29/06/2015	36.46	123.03
Brazil Ranch	30/06/2015	36.52	122.01
Pt Sur	30/06/2015	36.24	121.89
Conception	13/08/2015	34.50	120.60
Ventura	13/08/2015	34.23	119.37
Avila	14/08/2015	35.10	120.72
Cambria	14/08/2015	35.55	121.17
Canyon Axis (Red 1)	15/08/2015	36.66	122.46
Long Marine Lab	15/08/2015	36.92	122.04
Montara	15/08/2015	37.53	122.57
Blue Max 1	16/08/2015	38.00	126.18
Red Max 2	16/08/2015	38.00	125.00
Bodega	17/08/2015	38.31	123.13
Pepperwood	17/08/2015	38.57	123.43
Eureka Shelf	18/08/2015	40.83	124.36
Shelter Cove	18/08/2015	40.00	124.15
Blue Max 2	19/08/2015	41.05	126.50
Red Max 3	19/08/2015	42.50	126.00
Coos Bay	20/08/2015	43.45	124.46
Port Orford	20/08/2015	42.67	124.53
Florence	21/08/2015	44.00	124.46
Newport	21/08/2015	44.55	124.35